Doctoral Dissertation

Study on Air-Water Interface Enhancer for Efficient Oxygen Transfer in Diffused Aeration System

曝気における効率的な酸素移動のための空気／水接触促進装置に関する研究

March, 2021

Passaworn Warunyuwong

Graduate School of Sciences and Technology for Innovation,

Yamaguchi University

Table of Contents

List of Figures

List of Tables

Acknowledgements

I would like to express my sincere gratitude to my supervisor, Professor Tsuyoshi Imai for his helpful guidance and support throughout this study. I want to extend my thanks to all committees, Professor Masahiko Sekine, Professor Takaya Higuchi, Professor Takashi Saeki and Associate Professor Tasuma Suzuki for their contribution in my defense. I am also grateful to professors in Eisei laboratory, Associate Professor Koichi Yamamoto, and Associate Professor Ariyo Kanno for their meaningful suggestions and comments during English seminar. I would like to thank Mr. Tetsuhiko Fujisato from Bubble Tank Co. Ltd. for providing the equipment for experiments. I am thankful to my friends and members in Eisei laboratory for their valuable contribution, not only about work but also about my life during my living in Japan. Finally, this work would have not been possible without support and encouragement from my family throughout the years of my study.

Abstract

In wastewater treatment plants, an aeration system is considered as an important unit in biological treatment for supplying oxygen needed by microorganisms, providing dissolved oxygen distribution, and removing undesirable dissolved gases produced by biomass. In diffused aeration system, oxygen can dissolve into water through the bubble dispersion under water and the free water surface contacting atmospheric air. The bubble dispersion normally contributes to a larger proportion of overall oxygen transfer in comparison with water surface transfer. From the literature reviews regarding gas dissolution from the free surface, more than 10 % of overall mass transfer was contributed from free surface transfer. Therefore, the atmospheric oxygen transfer in an aeration tank designated with a large free surface area should be taken into consideration as well. However, in some situations, available spaces for the aeration tank construction are limited so that the diffused aeration process in such tanks can only rely on bubble dispersion. Therefore, it comes to an idea to improve the oxygen transfer into the water by increasing the contact area between air and water from the free surface transfer which is the main subject to study in this dissertation.

The objective of this work is to study about the feasibility of oxygen transfer improvement by an apparatus called air-water interface enhancer which was designed for diffused aeration systems to increase the contact area between air and water along the depth of the aeration tank. Its function is to receive the bubble plume from a diffuser located under the apparatus, accumulate air, and generate the air-water interface inside the apparatus (which referred to as the inner interface). This part can increase the contact area between air and water, and extent contact time between air and water through the air accumulation. The variables related to the study of upscaling effect were also determined to achieve empirical models which can estimate volumetric oxygen transfer coefficient and can be used as guidelines for designing the aeration system.

The objective was accomplished by conducting experiments in a lab-scale aeration tank and a pilot-scale aeration tank with adjustable water depth. In the lab-

scale aeration tank, the experiment was carried out to determine the optimal arrangement of the air-water interface enhancer which was chosen based upon the volumetric oxygen transfer coefficient and the standard oxygen transfer efficiency. Then the proportion of the oxygen transfer via different pathways and the enhancement of the specific interfacial area were investigated to understand the role of the apparatus. The effect of the diffuser submergence depth as well as the distance of the apparatus above the air diffuser on the oxygen transfer was also determined. By including results from the lab-scale aeration tank with the experiments in the pilot-scale aeration tank, upscaling of the application of apparatus was determined and data analysis was conducted by means of Solver function in the Microsoft Excel software to propose empirical models for estimating volumetric oxygen transfer coefficient. Finally, the horizontally additional installation of the apparatus was investigated for favorable operating conditions and empirical model development for aeration process with multiple aeration units.

The study on air-water interface enhancer for oxygen transfer improvement can be concluded as follows :

- A single layer of the air-water interface enhancer located near the water surface was the optimal arrangement which could improve the oxygen transfer process.
- The air-water interface enhancer increased contact between air and water not only by the presence of the inner interface but also by the air accumulation inside the apparatus.
- The oxygen transfer enhancement by the assistance of the air-water interface enhancer was possible in the deep aeration tank when the extent of air flow rate was sufficiently high for providing good mixing condition.
- Two empirical models developed as guidelines for designing diffused aeration system indicated that the air-water interface enhancer effectively improved the oxygen transfer at high air flow rate. They were also established that the effectiveness decreased with cross-sectional area of the aeration tank, but increased with water depth, diffuser submergence depth, and distance of the apparatus above the diffuser.

- The oxygen transfer improvement was possible in a deep, large aeration tank at high air flow rate when more than one aeration unit (an air diffuser equipped with an air-water interface enhancer) was applied providing significantly high degree of oxygen transfer performance, efficiency, and enhancement.
- The empirical models for aeration process with multiple aeration units were also proposed as design guidelines. However, the additional experiments were also recommended for more precise estimation.

Chapter 1 - Introduction and literature reviews

1.1 Aeration System

In wastewater treatment plants, an aeration system is a crucial unit process in biological operation. Its operation usually accounts up to 60-70 % of the total energy consumption at the plant. The principal role of aeration is (1) to supply sufficient amount of oxygen needed by respiration of microorganisms, (2) to ensure water circulation, which consequently provides uniform dissolved oxygen distribution in aeration tanks, and (3) to strip excess dissolved gases produced by biomass from biological processes, such as carbon dioxide (CO_2) and nitrogen (N_2).

There are two main categories of aeration systems which are diffused aeration system and mechanical aeration system. Diffused aeration is defined as oxygen transfer by the injection of oxygen-enriched air by submerged diffusion system. Oxygen transfer and mixing occurs as air bubbles rise to the surface from the porous or nonporous diffusers located under water. Mechanical aeration, on the other hand, is defined as water agitation and mixing by mechanical devices to cause the movement of water surface allowing transfer of oxygen from atmospheric air to the water. Typical mechanical aerators are, for example, horizontal surface impellers and vertical submerged impellers. In this present dissertation, the diffused aeration system was the main subject in the oxygen transfer enhancement.

Water in diffused aeration systems generally contacts oxygen in the gas phase via two pathways causing the oxygen dissolution, bubble transfer and free surface transfer. The former is the transfer through thin film of bubbles dispersing from bubble distributors. The bubble plume ascends to water surface by buoyant forces and consequently develops the latter oxygen transfer pathway. Oxygen from the atmosphere dissolved into the water through the air-water interface situated on the free water surface due to the turbulence induced by bubble motion and water circulation. The bubble dispersion normally contributes to a larger proportion of overall oxygen transfer in comparison with water surface transfer [1–4]. However, the free water

surface transfer in an aeration tank designated with a large water surface area should be taken into consideration as well [5].

1.2 Free water surface oxygen transfer

In physics, a free surface is the surface of a fluid that is subject to zero parallel shear stress, such as the interface between two homogeneous fluids [6], for example, the water and the atmospheric air. In hydrodynamics, a free surface is defined as the upper surface of a layer of liquid at which the pressure on the liquid is equal to the external atmospheric pressure [7]. In the aeration process, the free surface of water can allow molecules of oxygen from the atmosphere to transfer into the water.

There are many literatures concerning about gas transfer through the free surface or surface transfer of the liquid (*Table 1*). McWhirter and Hutter (1989) discovered that bubble oxygen transfer, which increased with air flow rate, was 5-8 times higher than surface oxygen transfer for fine bubble system, and 2-3 times higher for coarse bubble system [1]. Wilhelms and Martin (1992) reported that about one-third of the total oxygen transfer came from the free surface transfer, and the rest resulted from bubble transfer [2]. DeMoyer et al. (2003) indicated that the free surface transfer coefficient in a deep aeration tank was 59-85 % of the bubble transfer coefficient or about 40 % of the total volumetric oxygen transfer coefficient in average [3]. Moreover, Shibata et al. (2016) estimated that the free surface transfer was from 40 % up to 70 % of overall oxygen transfer in an aeration tank [5]. Schaub and Pluschkell (2006) revealed by correlations that the ratio of mass transfer on the free water surface to total mass transfer declined with air flow rate, 12-37 % for large nozzle diameter and 16-47 % for small nozzle diameter [4]. These mentioned studies suggested that the proportion of the free surface transfer is not too small to be overlooked, especially in the aeration tanks with large free surface areas. However, in some situations, available spaces for the aeration tank construction are limited so that the diffused aeration process in such tanks can only rely on bubble transfer. Therefore, it comes to an idea to improve the oxygen transfer into the water by increasing the contact area between air and water from the free surface transfer.

Table 1 Literatures related to free surface transfer.

References	Free surface transfer to total transfer ratio	Diffuser	Reactor	Gas flow rate
McWhirter and Hutter (1989) [1]	0.11 ~ 0.17	Fine bubble diffuser	Rectangular tank with a surface area of 37.2 m^2 and 3.05 ~ 7.62 m water depth	2.09 ~ 7.71 m^3/min
	0.25 ~ 0.33	Coarse bubble diffuser		3.55 ~ 11.39 m^3/min
Wilhelms and Martin (1992) [2]	0.33	23 cm diameter flexible head diffuser	Rectangular tank with 13 m width, 2.6 m length, and 1.1 m depth	18.9 LPM
DeMoyer et al. (2003) [3]	0.36 ~ 0.44	Coarse bubble diffuser with bubble diameter of 3 ~ 6 mm	Cylindrical tank with a diameter of 7.6 m and 9.6 m depth	51 and 78 m^3/hr
Schaub and Pluschkell (2006) [4]	0.12 ~ 0.37	4 mm diameter nozzle	Vessel with a diameter of 0.63 m and 0.57 m depth	6 ~ 48 LPM
	0.16 ~ 0.47	1 mm diameter nozzle		
Shibata et al. (2016) [5]	0.40 ~ 0.70	Porous polyurethane with bubble diameter of 1 mm	Rectangular tank with 5 m width, 5 m length, and 5 m depth	1.45 ~ 3.48 m^3/min

Moreover, there are groups of researchers focusing on the surface transfer improvement in diffused aeration system by using an apparatus called liquid-film-forming apparatus (*Figure 1*), which consists of a cone-shaped capture part as a bubble collector and an effluent part at the top of the cone [8–12]. They reported that the apparatus could enhance the overall oxygen transfer efficiency 11 to 37 % depending on water depth, water surface area, water volume, air flow rate, and diffuser type (also referred as generated bubble size). Although these studies concerned mainly with the improvement of oxygen transfer on the free water surface of the aeration tank, Jamnongwong et al. (2016) also indicated that the bubble collection phenomenon within the apparatus also had the role for oxygen transfer enhancement in terms of increasing interfacial area and prolonging contact time between bubbles and water [12].

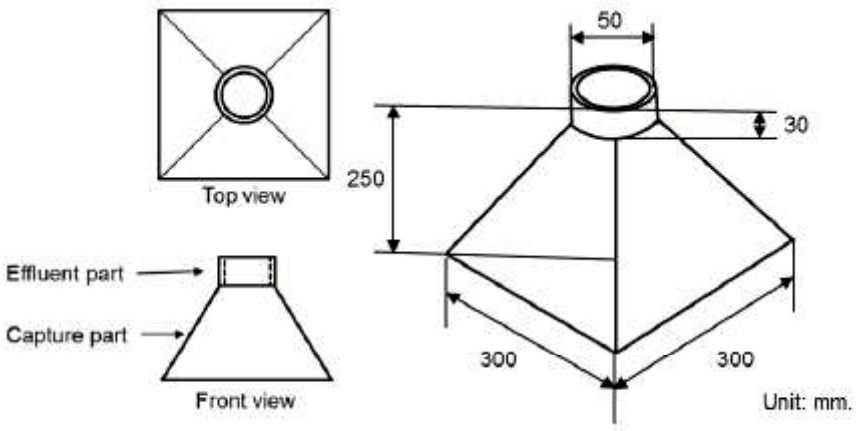

Figure 1 Liquid-film-forming apparatus (LFFA) [12].

1.3 Air-water interface enhancer

To emphasize on the oxygen transfer enhancement from water surface transfer, the author proposed an apparatus called air-water interface enhancer in this study. This apparatus was initially designed for oxygen transfer enhancement by increasing the contact area between air and water along the depth of the aeration tank. The air-water interface enhancer is made of plastic designed by a collaboration of Yamaguchi University and Bubble Tank Co., Ltd, Japan (*Figure 2*). *Figure 3* shows how the apparatus works. Its function is to receive the bubble plume from a diffuser located

under the apparatus, accumulate air, and generate the air-water interface inside the apparatus (hereafter referred to as the inner interface). This part can increase the contact area between air and water, accounting for approximately 0.1 m^2, and extent contact time between air and water through the air accumulation. After the inner interface is generated, the excess air is released through the tubes with 2.3 cm in diameter on the top of the apparatus. The apparatus can be installed above one another with the adjustable distance so that the additional inner interface can be expected.

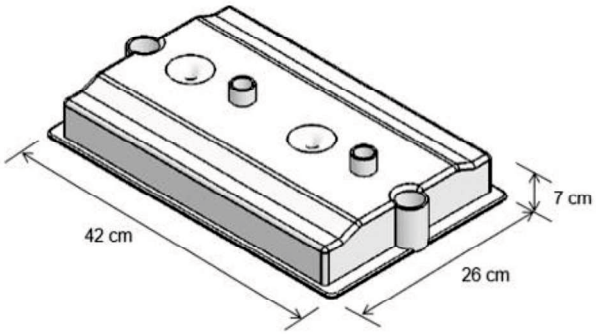

Figure 2 Air-water interface enhancer.

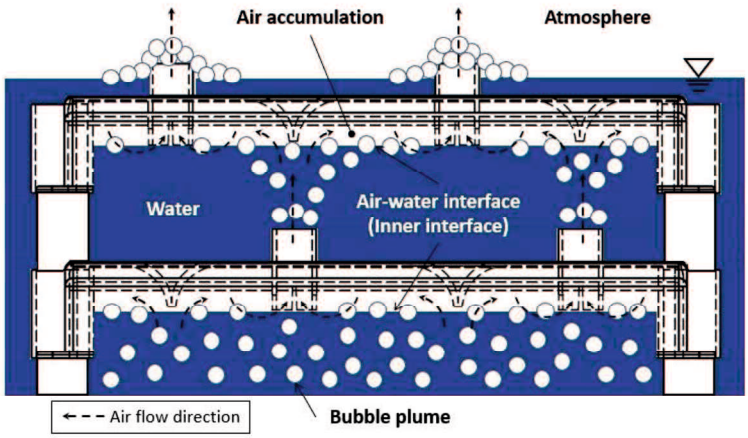

Figure 3 Illustrative representation of the working principle of air-water interface enhancer.

The application feasibility of the air-water interface enhancer was discussed in this dissertation by focusing the oxygen transfer performance and the oxygen transfer efficiency. Moreover, factors related to the diffused aeration process, which contribute to operating condition, are also examined in this study.

1.4 Diffuser submergence and tank geometry

When evaluating an aeration system, many factors can affect the oxygen transfer performance and efficiency. For diffused air systems these factors include diffuser type, diffuser placement, diffuser density, gas flow rate per diffuser or unit area, tank geometry and diffuser submergence, wastewater and environmental characteristics, etc [13]. These factors all have an important influence on the performance of the system. However, the relationship between these factors and the aeration performance and efficiency is not simple and may be difficult to understand. Therefore, they must be thoroughly considered in effective design of the aeration system. In this proposed dissertation, the diffuser submergence (as the position of the air diffuser) and the tank geometry (as the water volume and the water depth) were investigated together with the application of the air-water interface enhancer.

The submergence depth of diffusers can cause both positive and negative effects on oxygen transfer process. Typically, the diffuser submergence leads to the high hydrostatic pressure, which in turn, causes the high partial pressure of oxygen. The hydrostatic pressure is based on the distance from the water surface to the air-released point of the diffuser. The high partial pressure of oxygen allows the great driving force for the gas absorption process. Moreover, the saturated concentration of oxygen (and other gases contained in air) increases proportional to this pressure growth. The position of the diffusers is assumed to be above the floor of the aeration tank in conventional diffused aeration systems and should be near the floor of the aeration tank, as this will result in the higher hydrostatic pressure. The distance of bubble dispersion also causes long residence time of bubbles contacting with the water. These mentioned conditions are beneficial to the oxygen transfer process.

Even though the submergence depth has a positive effect on oxygen transfer, there are still some possible disadvantages. As the hydrostatic pressure created by the depth of water above the diffusers increases, the discharge pressure required at the air pumps for overcoming the pressure from water and driving air through the diffusers also increases. Therefore, power consumption and energy cost are highly required [14]. Moreover, as mentioned earlier, not only does the saturated concentration of oxygen increase due to the pressure rise, but the saturated concentrations of the other gases

generated in the process, such as CO_2 and N_2, also enhance resulting in the competition of the gas dissolution against oxygen. The supersaturation of these undesirable gases can also damage the aeration system in the activated sludge process since these gases may remain in the tank effluent and lead to partial solid flotation in the secondary sedimentation tank.

In this study, the tank geometry is referred to the size of the aeration tank (or the water volume) and the depth of the tank (or the water depth). The size of the tank is used to estimate the distribution of oxygen, whereas the depth of the tank is somewhat related to the diffuser submergence depth when the air diffuser is placed adjacent to the floor of the aeration tank.

Several investigations have studied the impact of factors which are related to the tank geometry, such as the liquid height, the liquid surface area, and the liquid volume, on the gas dissolution process. These factors contribute to the gas transfer into liquid phase in terms of volumetric mass transfer coefficient ($k_L a$). Yoshida and Akita (1965) reported that, in the column reactor, the $k_L a$ did not depend on the liquid height from 90 to 350 cm. However, an increasing of horizontal dimension of the liquid could improve the $k_L a$ [15]. The similar results were found in a study conducted by Kara et al. (1983). They indicated the relationship between the $k_L a$ and the ratio of liquid height to reactor diameter implying the $k_L a$ increased as whether decreasing liquid height or increasing horizontal area of liquid [16]. Moreover, Bavarian et al. (1991) mentioned that the changes in $k_L a$ by the liquid height also depended on superficial velocity. At superficial velocity below 70 m/hr, increasing liquid height could decrease $k_L a$. However, the effect of liquid height on the $k_L a$ was not found when the superficial velocity was over 70 m/hr [17]. Yet, Wu and Hsuin (1996) revealed the contradictory results. The low liquid height showed less $k_L a$ values than those in high liquid height due to short gas-liquid contact time in the reactor with low superficial air velocity. Noted that liquid height is directly proportional to liquid volume when liquid surface area is uniform [18]. Chang and Morsi (1992) reported that $k_L a$ values decreased with increasing liquid volume. Additionally, when the liquid height increased, the hydrostatic pressure on gas bubbles also increased which reduced the gas bubble size [19]. The similar reports were also described in the literature by Leu

et al. (1998). The liquid height caused the difference in the liquid volume, the hydrostatic pressure, and the rising distance of air bubbles. They revealed that increasing liquid height up to 175 cm diminished $k_L a$ as liquid volume increased. However, at the liquid height more than 175 cm, the $k_L a$ increased because of the increment of both hydrostatic pressure and rising distance of air bubbles [20]. The liquid physical properties also have some impact. Bando et al. (2003) found that the effect of liquid height on the $k_L a$ depended on the viscosity of liquid. In case of low viscous liquid or tap water, $k_L a$ increased with increasing liquid height. On the contrary, in case of highly viscous liquid, $k_L a$ decreased with increasing liquid height and became constant beyond a certain height [21].

1.5 Analytical oxygen transfer parameters

1.5.1 Volumetric oxygen transfer coefficient

To evaluate oxygen transfer performance, the standard parameter for testing is the volumetric oxygen transfer coefficient ($k_L a$), which its calculation method follows the ASCE Standard for Measurement of Oxygen Transfer in Clean Water [22]. It is the most common parameter used in the field of gas-liquid transfer research.

The volumetric oxygen transfer coefficient, $k_L a$, is the product of the liquid side mass transfer coefficient, k_L and the interfacial area exposed to transfer in given liquid volume or the specific interfacial area, a. However, the individual values of k_L and a are quite impossible to individually measure from experiments. Combining them into one term as $k_L a$ is much easier to obtain as a measurable parameter in aeration systems [13].

By assuming thoroughly mixed body of clean water at any instant of time, the oxygen mass transfer rate, which is dependent upon the volumetric oxygen transfer coefficient and the driving force due to the difference between saturated concentration and dissolved concentration in bulk liquid, is often expressed as follows [13,22–24].

Equation 1

$$\frac{dC}{dt} = k_L a(C_S - C)$$

where $\frac{dC}{dt}$ is the oxygen accumulation rate, $k_L a$ is the volumetric oxygen transfer coefficient, C_S is the saturated dissolved oxygen concentration, and C is the dissolved oxygen concentration in water.

By rearranging *Equation 1* and integrating within the proper limits, *Equation 2* can be obtained.

Equation 2 $$ln\left(\frac{C_s - C_0}{C_s - C_t}\right) = k_L a \cdot t$$

where C_0 is the initial dissolved oxygen concentration in water at time $t = 0$, and C_t is the dissolved oxygen concentration in water at time t.

By plotting a graph of *Equation 2* where t and $ln\left(\frac{C_s - C_0}{C_s - C_t}\right)$ are indicated as x-axis and y-axis, respectively. Hence, the slope of the graph can be estimated as the $k_L a$.

The change in temperature affects the diffusivity of oxygen and the liquid side mass transfer coefficient [13]. Therefore, the obtained $k_L a$ is calibrated to the value at a standard reference temperature of 20 °C.

Equation 3 $$k_L a_{(20)} = k_L a_{(T)} \times 1.024^{(20-T)}$$

where $k_L a_{(20)}$ and $k_L a_{(T)}$ are the $k_L a$ at 20 °C and the actual operating temperature of T °C, respectively.

1.5.2 Standard oxygen transfer rate

The standard oxygen transfer rate ($SOTR$) is the mass of oxygen transferred into a given volume of liquid per unit time at standard conditions.

Equation 4 $$SOTR = k_L a_{(20)} C_{s(20)} V$$

where $SOTR$ is in [kg/s], $k_L a_{(20)}$ is in [s^{-1}], $C_{s(20)}$ is the saturated concentration of oxygen at 20 °C, in [kg/m^3], and V is the water volume, in [m^3]. The saturated concentration of oxygen at 20 °C is typically around 9.09 mg/L.

1.5.3 Standard oxygen transfer efficiency

The standard oxygen transfer efficiency ($SOTE$) is the ratio of the standard oxygen which is actually transferred or dissolved into the liquid and the standard oxygen supplied to the aeration system.

Equation 5

$$SOTE = \frac{SOTR}{\rho_g W_{O_2} Q_g} \times 100$$

where $SOTE$ is in [%], ρ_g is the density of air under standard condition, in [kg/m^3], W_{O_2} is the weight fraction of oxygen in air, in [kg O_2/kg air], and Q_g is the air flow rate, in [m^3/s]. The density of air at 20 °C is 1.293 kg/m^3, and the weight fraction of oxygen in air is 0.2315 kg O_2/kg air.

1.5.4 Standard aeration efficiency

The standard aeration efficiency (SAE) is the rate of oxygen transfer per unit power input. It represents the efficiency in terms of energy consumption.

Equation 6

$$SAE = \frac{SOTR}{P} \times 3600$$

where SAE is in [kg/kwh], and P is the power input of air pump, in [kW].

1.6 Thesis objectives

The key goal of this dissertation is to study about the feasibility and utility of the air-water interface enhancer for effective improvement of oxygen transfer performance and efficiency. To do so, the secondary objectives are to

(1) investigate for optimal arrangement of the air-water interface enhancer for effective oxygen transfer improvement in the laboratory scale

(2) determine the role of the air-water interface enhancer on the improvement of volumetric oxygen transfer coefficient and specific interfacial area

(3) study the effect of factors related to the diffused aeration process with the application of the air-water interface enhancer

(4) propose the empirical models for determining volumetric oxygen transfer coefficient as design guidelines

(5) investigate the effect of the additional aeration unit with the application of air-water interface enhancer on oxygen transfer performance, efficiency, and improvement.

1.7 Thesis overview

The present dissertation was to study the feasibility and utility of the proposed air-water interface enhancer to improve the aeration transfer process. A series of experiments (Chapter 2-5) were conducted to examine the application of the air-water interface enhancer, understand the role of the air-water interface enhancer, develop empirical models for the single apparatus application, and determine the effect of the number of aeration unit.

In Chapter 2, the experiment was conducted to determine the optimal arrangement of the air-water interface enhancer. The optimal arrangement was chosen based upon the volumetric oxygen transfer coefficient and the standard oxygen transfer efficiency. It was initially hypothesized that a greater number of apparatus installed in the aeration system would lead to larger air-water interface, hence the better oxygen transfer.

In Chapter 3, the experiment was conducted following the experiment in Chapter 2 to determine the proportion of the oxygen transfer via different pathways, which are bubble transfer, inner interface transfer, and free water surface transfer. Moreover, the mathematical analysis was performed for specific interfacial area calculation to determine the enhancement of the interfacial area from the air-water interface enhancer.

In Chapter 4, as the optimal arrangement of the air-water interface enhancer and its role were achieved from Chapter 2 and Chapter 3, this chapter was aimed for the effect of the diffuser submergence depth as well as the distance of the air-water interface enhancer above air diffuser. This experiment was designed to determine the possibility to minimize the hydrostatic pressure in the system with the air-water

interface enhancer. Moreover, the tank geometry was also studied for upscaling and develop empirical models for estimating volumetric oxygen transfer coefficient in the aeration system equipped with the proposed air-water interface enhancer.

From Chapter 2 to Chapter 4, the application of the air-water interface enhance was merely investigated as a single aeration unit. In Chapter 5, the experiment, therefore, was conducted for determining the effect of the number of the aeration unit which was composed of an air diffuser and an air-water interface enhancer. This experiment was aimed for favorable condition of oxygen transfer in terms of oxygen transfer performance, oxygen transfer efficiency, and oxygen transfer enhancement by the presence of the air-water interface enhancer. Moreover, the empirical models based on models for single aeration unit from Chapter 4 were modified to the models for multiple aeration units.

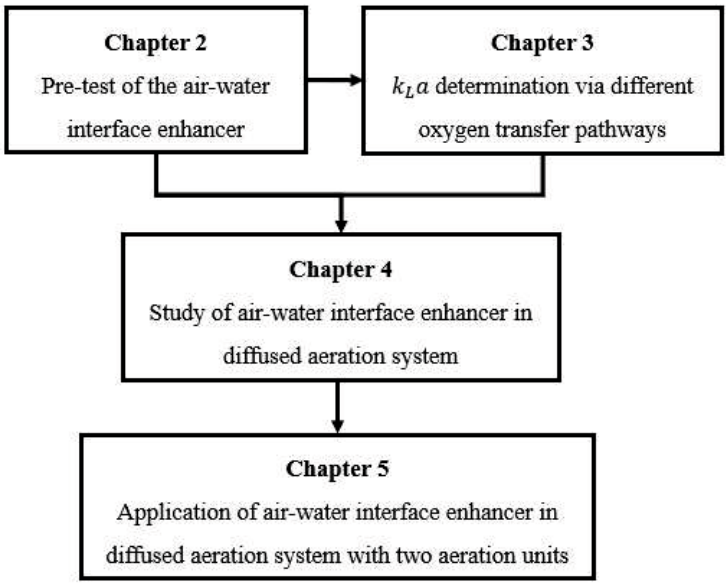

Figure 4 Overview of present dissertation.

Chapter 2 - Pre-test of the air-water interface enhancer

2.1 Introduction

The air-water interface enhancer was initially designed aiming to increase contact area between air and water by the presence of water surface inside the apparatus (inner interface) in diffused aeration systems. However, the appropriate use of this apparatus was still unknown. Therefore, the experiment was necessary to clarify that the proposed apparatus was effective in aeration process enhancement.

The objectives of this chapter were focusing to

(1) determine aeration performance and efficiency in terms of the volumetric oxygen transfer coefficient ($k_L a$) and the standard oxygen transfer efficiency ($SOTE$).

(2) find the optimal arrangement of the air-water interface enhancer by varying the gap between apparatus and diffuser, the number of apparatus, and the gap between apparatus.

(3) understand the mechanism of the arrangement of the air-water interface enhancer.

2.2 Materials and method

2.2.1 Experimental setup

In general, as shown in *Figure 5*, the experiments were carried out in a 30-cm width x 90-cm length x 55-cm height water tank (1) at the volume of 100 L of tap water (water density; $\rho_w \approx 997$ kg/m^3). A 3-cm in diameter x 30-cm long tubular air stone diffuser (2), which can produce air bubbles with a diameter of approximately 3–4 mm, was located at the bottom of the tank. An air pump (3) supplied gas phase of air (gas density; $\rho_g \approx 1.198$ kg/m^3, and oxygen content; $O_W \approx 0.232$) with an adjustable flow rate by a rotameter (4). The set of the air-water interface enhancer (5) was installed exactly above the diffuser. A DO meter with a response time of 30 s (Horiba OM-51) (6) was used for measuring dissolved oxygen concentration and water

temperature, and its probe (7) was placed at the middle of water depth as the represented point of average dissolved oxygen concentration in the aeration tank.

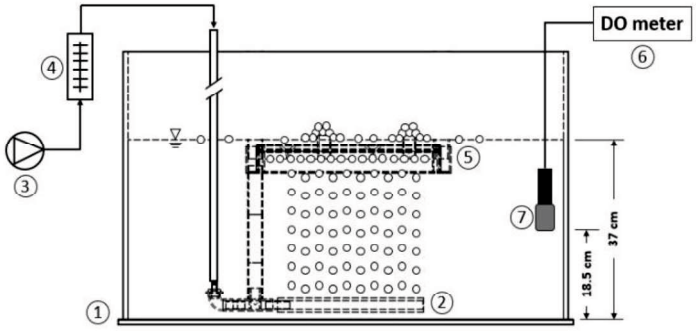

Figure 5 Experimental setup in general.

The investigation for the optimal arrangement of the air-water interface enhancer was varied by the number and the position of the apparatus, as shown in *Figure 6*. Due to the size of the experimental tank, the apparatus can be installed up to three layers with the minimum distance between each apparatus of 10 cm and the minimum distance of the apparatus above the diffuser of 10 cm. In consequence, the positions of the apparatus can be herein entitled as None, Bottom (B), Middle (M), Top (T), Bottom-Middle (BM), Bottom-Top (BT), Middle-Top (Middle-Top), and Bottom-Middle-Top (BMT). The air flow rates of 20 LPM and 100 LPM, which are within the range of the typical operation of the rigid diffuser type [23], was also observed.

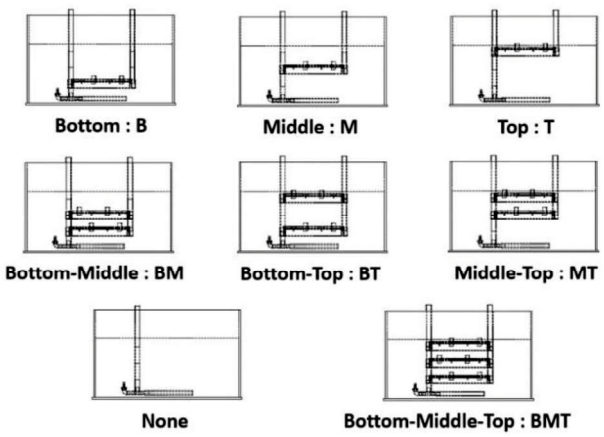

Figure 6 Experimental setups for determining the optimal arrangement.

2.2.2 Testing methodology

The oxygen transfer tests were conducted in accordance with ASCE Standard procedures for clean water [22]. The 100 mg/L of sodium sulfite solution with 1 mg/L of cobalt chloride catalyst was used to reduce dissolved oxygen concentration of tap water to nearly 0 mg/L at the start of each test. Then air was injected into the aeration tank, and the dissolved oxygen concentration and the water temperature were recorded continuously at an interval of 10 s for 20 to 30 min until the dissolved oxygen level in the water reached approximately 90 % of the presumed saturated value [25]. Then the volumetric oxygen transfer coefficient and the standard oxygen transfer efficient were determined followed the procedure in *1.5 Analytical oxygen transfer parameters.*

2.3 Results and discussion

Figure 7 shows the volumetric oxygen transfer coefficients obtained from the different arrangements in *Figure 6* at the air flow rates of 20 LPM and 100 LPM. It can be seen that the higher air flow rate provided the higher oxygen transfer performance because more bubbles were produced. Regarding the different arrangements, the trends were quite similar in both air flow rates. Normally, oxygen transfer performance in the diffused aeration mainly depends on bubble characteristics (i.e., bubble size distribution) [26,27] and mixing condition [27,28]. However, the oxygen transfer performance of some cases became worse when the apparatus was applied because bubbles could not freely disperse throughout the aeration tank.

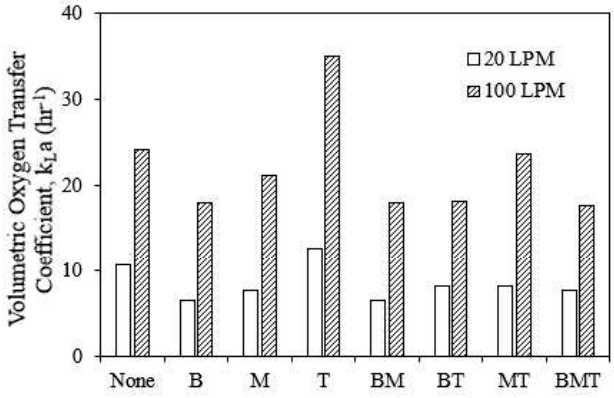

Figure 7 Comparison of volumetric oxygen transfer coefficient from different experimental arrangements.

Obviously, B, BM, BT, and BMT setups provided low volumetric oxygen transfer coefficients because bubble dispersion was obstructed at the beginning of bubble movement even though those cases had the inner interface from the air-water interface enhancer. M and MT setups more or less provided better results when compared to B, BM, BT, and BMT setups because there was more distance for bubble dispersion from the diffuser before passing through the apparatus. The highest volumetric oxygen transfer coefficient was obtained from Top setup, which can enhance oxygen transfer performance beyond the conventional diffused aeration. This is due to the maximum available depth for bubble dispersion, which allowed small bubbles to freely disperse at the distance similar to the none-device setup, and the assistance from the inner interface transfer in promoting the overall oxygen transfer.

Figure 8 shows the comparison of bubble dispersion from different arrangements. It is also noticeable that the travelling distance of bubble plume released directly from the diffuser (A in *Figure 8*) was shortened when the air-water interface enhancer was installed. After the plume was released from the apparatus through the tubes, the plume became narrow bubble currents with larger bubbles (B in *Figure 8*), hence the poorer bubble scattering. Normally, large bubbles rise more rapidly than small bubbles [29]. Therefore, the contact time between air and water decreases, which in turn, lowering the oxygen dissolution. The apparatus obviously changed the flow regime of bubbles from homogeneous regime into slug bubble regime (*Figure 9*) due to the relatively high air flow rate and small diameter of the tubes [30]. Moreover, when slug bubbles ascended from one apparatus through the following above one, the bubble intensity was depleted as well as the water turbulence on the free water surface. As a result, there was decrease of overall oxygen transfer even though the more numbers of contact areas between gas phase and liquid phase were generated.

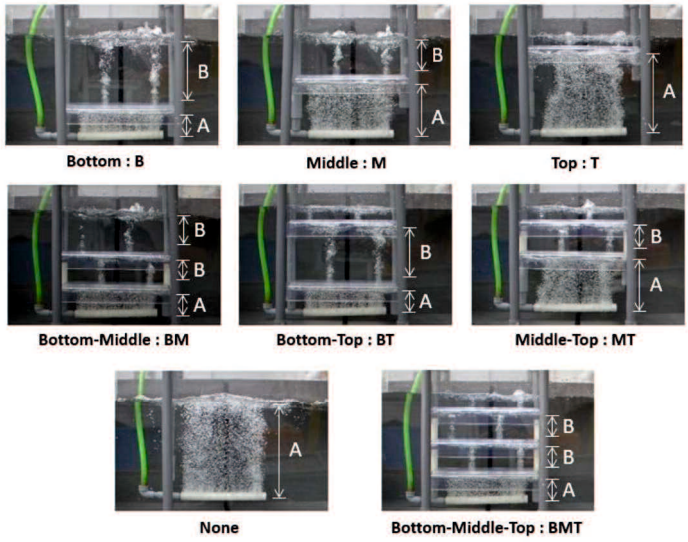

Figure 8 Comparison of bubble dispersion from different experimental arrangements.

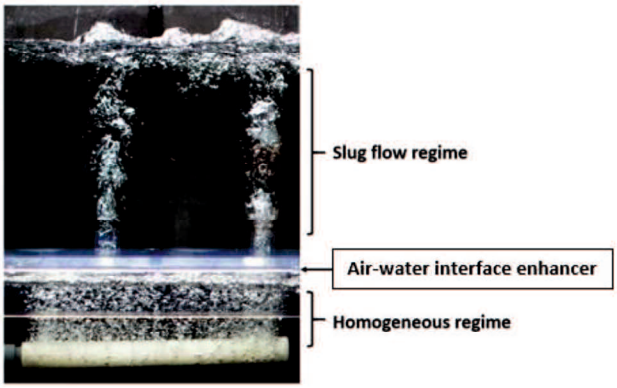

Figure 9 Bubble flow regimes before and after passing through the apparatus.

Figure 10 shows the standard oxygen transfer efficiency obtained from the different arrangements in *Figure 6* at the air flow rates of 20 LPM and 100 LPM. Similar to the case of volumetric oxygen transfer coefficient, the highest $SOTE$ was obtained from Top setup, which can enhance the oxygen transfer efficiency beyond the conventional diffused aeration. However, the contradiction was found when the air flow rate was considered. The $SOTE$ values at 20 LPM were higher than those at 100 LPM. This indicated that oxygen was effectively dissolved into water at lower air flow rate whereas the excess amount of oxygen at higher air flow rate was lost to the atmosphere when the air reached the water surface.

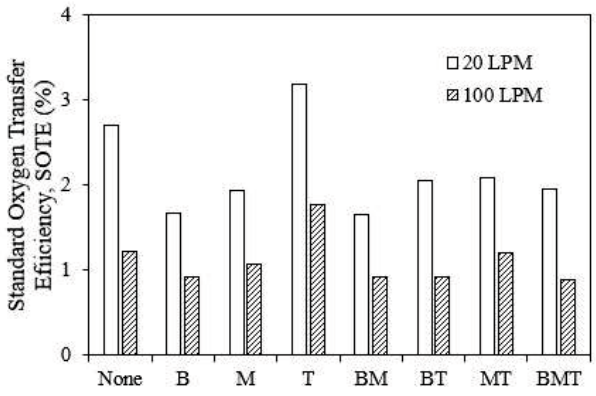

Figure 10 Comparison of standard oxygen transfer efficiency from different experimental arrangements.

2.4 Conclusion

From the results of the preliminary experiment, a single layer of the air-water interface enhancer placed near the water surface was the best setup that could improve oxygen transfer performance and efficiency. Due to the available distance for bubble dispersion, bubbles could freely disperse, and the assistance from inner interface transfer could promote the overall oxygen transfer process. Therefore, it should be taken into consideration that the apparatus should be located where bubble transfer provides the most effectiveness. It was also found that the volumetric oxygen transfer coefficients of the air flow rate at 100 LPM were up to 3 times higher than those at 20 LPM. However, when comparing the $SOTE$, oxygen could be effectively transferred at 20 LPM. The excess amount of oxygen at 100 LPM was lost to the atmosphere when the air reached the water surface.

Finally, the mechanism of the air-water interface enhancer could imply that the oxygen transfer process in this study depended on three sub-processes regarding to oxygen transfer pathways which were bubble transfer, oxygen transfer inside the apparatus, and oxygen transfer from atmosphere on water surface. Each process had different significant proportion on the overall oxygen transfer which would be further discussed in the next chapter.

Chapter 3 - $k_L a$ determination via different oxygen transfer pathways

3.1 Introduction

In previous chapter, the results indicated that it was possible to effectively improve oxygen transfer performance and efficiency when the appropriate arrangement of the air-water interface enhancer and air flow rate were applied. However, its function in detail has to be more investigated. In this chapter, the author conducted the experiment to clarify the role of the apparatus. In order to understand the role of the apparatus, the overall oxygen transfer was divided corresponding to pathways where the oxygen transfer occurred; from bubbles, from water surface inside the apparatus (inner interface), and from free water surface (*Figure 11*). The aeration processes, with and without the apparatus, were also compared to observe the effect of the apparatus. Moreover, the mathematical analysis was performed in terms of the specific interfacial area calculation to determine the enhancement of the interfacial area from the air-water interface enhancer.

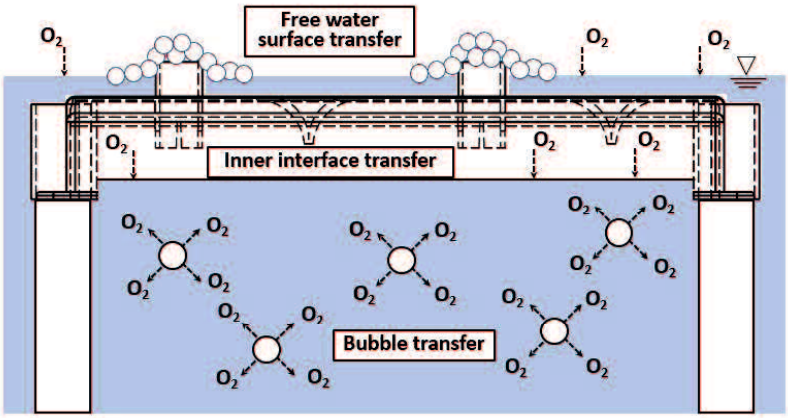

Figure 11 Diagram of oxygen transfer processes via different pathways.

The objectives of this chapter were to

(1) understand the role of the air-water interface enhancer by determining volumetric oxygen transfer coefficients from the pathways where oxygen transfer occurred.

(2) clarify the role of the air-water interface enhancer on the interfacial area by determining the experimental values of specific interfacial areas and compare them with the measured values.

3.2 Materials and method

3.2.1 Experimental setup

In general, the experiments were carried out in the identical setup as in Chapter 2 (*Figure 5*). The arrangement of the air-water interface enhancer was decided by the results from Chapter 2 which revealed that Top setup or a single layer of the apparatus near the water surface was the optimal arrangement for oxygen transfer enhancement. Therefore, this arrangement was set as the experimental setup for this investigation.

The determination for the effect of the air-water interface enhancer on individual oxygen transfer pathways was tested by covering the interfaces where oxygen transfer process occurs with 10-mm thick Styrofoam sheets to eliminate the oxygen transfer [3,31] (*Figure 12*). For example, if the Styrofoam sheet is placed on free water surface, the free water surface transfer is limited, likewise, if the Styrofoam sheet is placed on water surface inside the apparatus, the inner interface transfer is limited. The Styrofoam sheets were perforated to prevent gas accumulation in the water by releasing excess air, which does not transfer into the water. As a result, the oxygen transfers across the free water surface, the inner interface, and the bubble transfer can be estimated individually.

Figure 12(a-1) and *Figure 12*(a-2) represent the experimental setups of conventional diffused aeration, without and with Styrofoam sheet, respectively. *Figure 12*(b-1) and *Figure 12*(b-2) represent the example of the experimental setups equipped with the air-water interface enhancer, without and with Styrofoam sheets, respectively. The air flow rate used for these tests was 20 LPM.

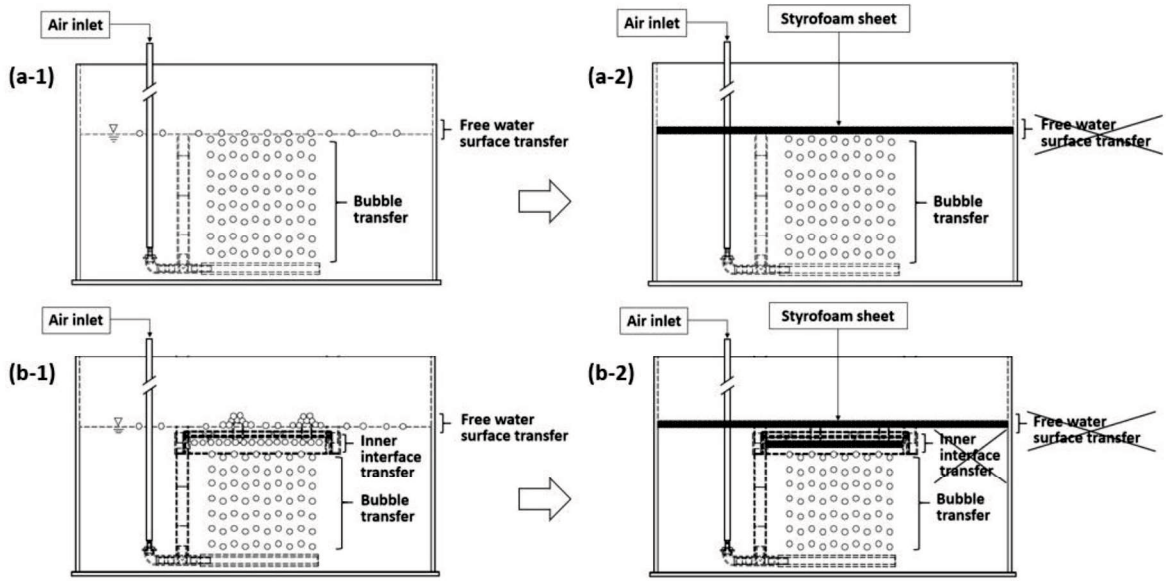

Figure 12 Experimental setup with Styrofoam sheets.

3.2.2 Testing methodology

The oxygen transfer tests were conducted in accordance with ASCE Standard procedures for clean water [22]. The 100 mg/L of sodium sulfite solution with 1 mg/L of cobalt chloride catalyst was used to reduce dissolved oxygen concentration of tap water to nearly 0 mg/L at the start of each test. Then air was injected into the aeration tank, and the dissolved oxygen concentration and the water temperature were recorded continuously at an interval of 10 s for 20 to 30 min until the dissolved oxygen level in the water reached approximately 90 % of the presumed saturated value [25]. Then the volumetric oxygen transfer coefficient was determined followed the procedure in *1.5 Analytical oxygen transfer parameters*.

When conventional diffused aeration is operated, there are two primary interfaces where oxygen can be transferred, a bubble-water interface from dispersed bubbles (bubble transfer) and an air-water interface from the atmosphere on the free water surface (free water surface transfer). Thus, the total volumetric oxygen transfer coefficient can be assumed as the sum of volumetric oxygen transfer coefficients from both contact interfaces as follows.

Equation 7 $$k_L a_T = k_L a_B + k_L a_S$$

where $k_L a_T$ is the total volumetric oxygen transfer coefficient, $k_L a_B$ and $k_L a_S$ are the volumetric oxygen transfer coefficients for bubble transfer and free water surface transfer, respectively.

In this study, the air-water interface enhancer was applied to generate the additional air-water interface, namely inner interface. Therefore, the total volumetric oxygen transfer coefficient, in this case, can be expressed as the sum of three coefficients as follows.

Equation 8 $$k_L a_T = k_L a_B + k_L a_I + k_L a_S$$

where $k_L a_I$ is the volumetric oxygen transfer coefficient for inner interface transfer.

Moreover, *Equation 8* can be derived into *Equation 9* when the Styrofoam sheet was placed on free water surface, or into *Equation 10* when it was placed inside the apparatus, or into *Equation 11* when it was placed at both positions at the same time.

Equation 9 $$k_L a_T = k_L a_B + k_L a_I$$

Equation 10 $$k_L a_T = k_L a_B + k_L a_S$$

Equation 11 $$k_L a_T = k_L a_B$$

3.2.3 Mathematical analysis

In order to conduct mathematical analysis for determining the specific interfacial area enhancement from the air-water interface enhancer, the experimental values of specific interfacial areas were compared with the measured values. Moreover, the value of liquid side mass transfer coefficient (k_L) was also compared with the values found from the literature reviews to validate the analysis. The overall process is depicted as shown in *Figure 13*.

Specific interfacial area (a) is defined as interfacial area which air contacts water divided by water volume (*Equation 12*).

Equation 12 $$a = \frac{A}{V}$$

where A is the interfacial area, V is the water volume.

The interfacial area depends on the characteristic of air contacting water. The specific interfacial area of bubbles (a_B), the specific interfacial area of inner interface (a_I), and the specific interfacial area of free surface (a_S) are calculated from the surface area of bubbles (A_B), the surface area of inner interface (A_I), and the surface area of free water surface (A_S), respectively.

For the measured values of the specific interfacial area of inner interface ($a_{I,mea}$) and the specific interfacial area of free surface ($a_{S,mea}$) can be determined by measuring surface areas of inner interface and free water surface which then are applied in *Equation 12*. The following *Equation 13* and *Equation 14* can be obtained.

Equation 13 $$a_{I,mea} = \frac{A_I}{V}$$

Equation 14 $$a_{S,mea} = \frac{A_S}{V}$$

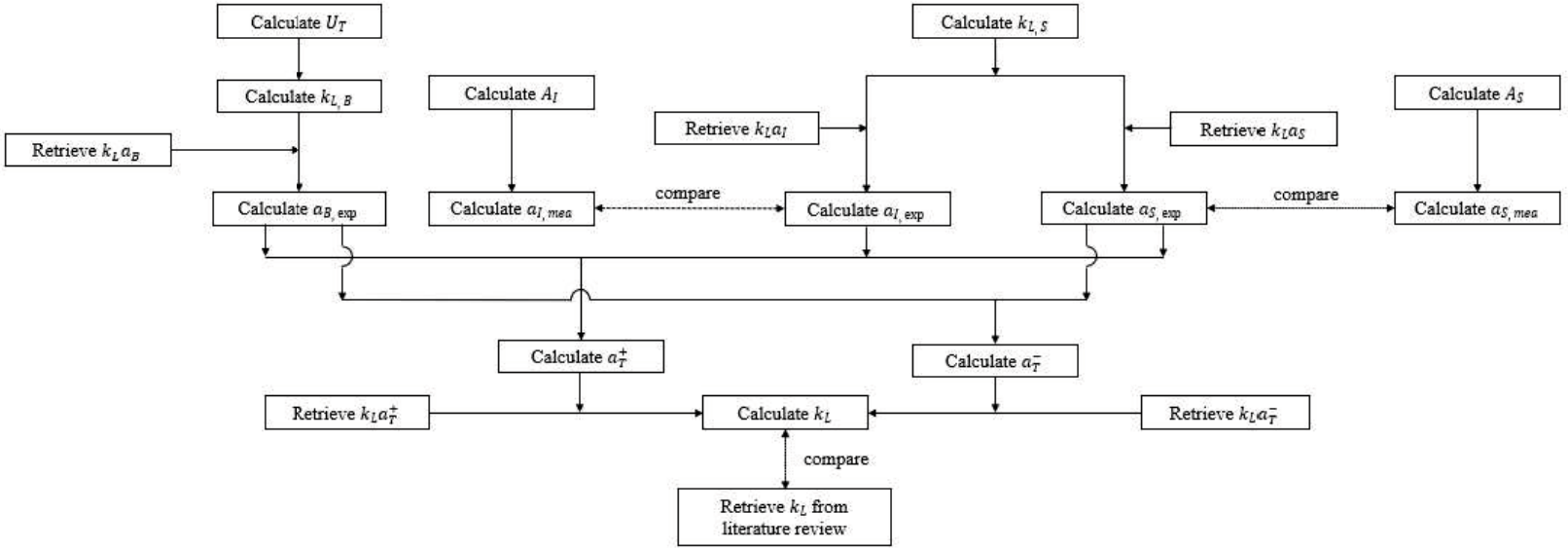

Figure 13 Overall process of the mathematical analysis for determining the specific interfacial area enhancement.

However, the surface area of bubbles dispersing in the aeration tank is difficult to obtain. Theoretically, the a_B value can be obtained by deriving *Equation 12* into *Equation 15.*

Equation 15 $$a_B = \frac{6\varepsilon_G}{d_B(1-\varepsilon_G)}$$

where ε_G is the gas holdup or the proportion of air in the aeration system. The amount of air contained in water during aeration process can be obtained by measuring the change of water level. The change of water level resulted from air introduction into water is not difficult to measure when the change of water level is significantly apparent, and the fluctuation of the water surface caused by water turbulence is less observed. Therefore, this measurement can be conducted in the diffused aeration system which possesses small water surface area such as in the bubble columns. However, the change of water level in the aeration tank with large free water surface area is relatively small and almost impractical to obtain. Therefore, the author did determine only the experimental values of the specific interfacial area of bubble ($a_{B,exp}$) which could be obtained by the following procedure.

First of all, the terminal rising velocity of single bubbles was estimated. Theoretically, the steady-state velocity of bubbles occurs when the buoyant force equals to the drag force on the bubbles and can be obtained when the bubble diameter is known. For the bubble diameter greater than 1.4 mm, the bubble terminal rising velocity can possibly be determined by following *Equation 16* [27,32,33].

Equation 16 $$U_T = \sqrt{\frac{2\sigma_L}{d_B\rho_L} + \frac{gd_B}{2}}$$

where U_T is the terminal rising velocity of single bubbles, σ_L is the surface tension of liquid, ρ_L is the density of liquid, g is the gravitational constant (g = 9.81 m/s^2), d_B is the equivalent bubble diameter. At standard condition with the temperature of 20 °C, σ_L and ρ_L of water are 7.2 x 10^{-2} kg/s^2 and 997 kg/m^3, respectively.

Next, the mass transfer coefficients were determined. There are two major types of mass transfer coefficient categorized by the characteristic of mass transfer pathways which are the bubble-water interface and the atmospheric air-water interface. In case of the mass transfer coefficient for bubble-water interface or the bubble mass transfer coefficient, it can be calculated by following Higbie's penetration theory [27,33–35].

Equation 17

$$k_{L,B} = 2\sqrt{\frac{DU_T}{\pi d_B}}$$

where $k_{L,B}$ is the bubble mass transfer coefficient, D is the diffusion coefficient. The diffusion coefficient of oxygen in water is approximately 2.01 x 10^{-9} m^2/s at 20 °C [36,37].

Finally, the experimental value of the specific interfacial area of bubble ($a_{B,exp}$) was calculated by the experimental value of $k_L a_B$ and the value of $k_{L,B}$ as follows.

Equation 18

$$a_{B,exp} = \frac{k_L a_B}{k_{L,B}}$$

For the mass transfer coefficient for atmospheric air-water interface or the surface mass transfer coefficient, it includes all water surface areas contacting the atmospheric air. The extent of water surface mass transfer is generally controlled by the turbulence near the water surface and will be highly enhanced in strong turbulence. To estimate the surface mass transfer coefficient, the following *Equation 19* was used [34,38–40].

Equation 19

$$k_{L,S} = \frac{c(\varepsilon v_L)^{0.25}}{Sc^{0.5}}$$

where $k_{L,S}$ is the surface mass transfer coefficient, c is the small eddy model (SEM) coefficient, ε is the turbulent energy dissipation rate on the water side close to the free surface, v_L is the kinematic viscosity, and Sc is Schmidt number ($Sc = v_L/D$). At 20 °C, the kinematic viscosity of water is 1.004 x 10^{-6} m^2/s.

The inner interface and the free water surface can be defined as the surface area which contacts the atmospheric air, and its mass transfer is generally controlled by the turbulence near the water surface. Therefore, the $k_{L,S}$ was applied for determining both experimental values of the specific interfacial area of inner interface ($a_{I,exp}$) and free water surface ($a_{S,exp}$) as shown in *Equation 20* and *Equation 21*.

Equation 20
$$a_{I,exp} = \frac{k_L a_I}{k_{L,S}}$$

Equation 21
$$a_{S,exp} = \frac{k_L a_S}{k_{L,S}}$$

Then the $a_{I,mea}$ and $a_{S,mea}$ values were compared with the $a_{I,exp}$ and $a_{S,exp}$ values, respectively.

To determine the value of liquid side mass transfer coefficient (k_L), the specific interfacial area obtained from the aeration tank with the apparatus (a_T^+) and the specific interfacial area obtained from the aeration tank without the apparatus (a_T^-) were calculated from *Equation 22* and *Equation 23.*

Equation 22
$$a_T^+ = a_{B,exp} + a_{I,exp} + a_{S,exp}$$

Equation 23
$$a_T^- = a_{B,exp} + a_{S,exp}$$

Then the value of liquid side mass transfer coefficient (k_L) was calculated by following *Equation 24* and *Equation 25*, and was compared from the literature reviews.

Equation 24
$$k_L = \frac{k_L a_T^+}{a_T^+}$$

Equation 25
$$k_L = \frac{k_L a_T^-}{a_T^-}$$

where $k_L a_T^+$ and $k_L a_T^-$ are the total oxygen transfer coefficients obtained from the experiments with and without the air-water interface enhancer, respectively.

3.3 Results and discussion

3.3.1 Oxygen transfer coefficient

Table 2 shows the experimental results and the calculation results derived from the experimental results. The X marks indicate that certain oxygen transfer pathways were limited by covering Styrofoam sheets. Under the normal operating condition without the air-water interface enhancer, the $k_L a_T$ value of 10.69 hr^{-1} can be observed while the test conducted with Styrofoam sheets covering the free water surface provided the $k_L a_T$ value of 9.32 hr^{-1}. In consequence, the $k_L a_B$ and the $k_L a_S$ values of 9.32 hr^{-1} and 1.37 hr^{-1}, respectively, can be simply calculated. It can be noticed that the oxygen transfer on the free water surface from the conventional aeration made up 12.8 % of the total oxygen transfer which nearly conform to the results from Zhu et al. (2007) at 9.4 % [8], Imai and Zhu (2011) at 10.7 % [10], and Jamnongwong et al. (2016) at 13 % [12]. When the apparatus was applied, the normal operating condition provided the $k_L a_T$ value of 12.61 hr^{-1} indicating the improvement of oxygen transfer beyond the test without the apparatus. The tests conducted with Styrofoam sheets covering the free water surface and the inner interface inside the apparatus showed lower $k_L a_T$values. In this case, there were four possible equations, however, there were only three variables needed to be solved. Therefore, the equations were grouped into four conditions to determine $k_L a_B$, $k_L a_I$, and $k_L a_S$ from each group (*Table 3*). As the results from the calculation, the average values of $k_L a_B$, $k_L a_I$, and $k_L a_S$ could be approximately obtained as 9.22 hr^{-1}, 1.94 hr^{-1}, and 1.40 hr^{-1}, respectively, accounting for 73.4 %, 15.4 %, and 11.2 % of the $k_L a_T$ value.

Table 2 Experiment and calculation results for $k_L a$ determination via different oxygen transfer pathways.

Experiment setups	Oxygen transfer pathway			Experiment result	Calculation result		
	Bubble transfer	Inner interface transfer	Free water surface transfer	$k_L a_T$ (hr^{-1})	$k_L a_B$ (hr^{-1})	$k_L a_I$ (hr^{-1})	$k_L a_S$ (hr^{-1})
Without apparatus	√	-	√	10.69	9.32 (≈87.2%)	-	1.37 (≈12.8%)
	√	-	X	9.32			
With apparatus	√	√	√	12.61	9.22 (≈73.4%)	1.94 (≈15.4%)	1.40 (≈11.2%)
	√	√	X	11.10			
	√	X	√	10.57			
	√	X	X	9.27			

Note: √ : available, - : unavailable, X : eliminated.

Table 3 Calculation for $k_L a$ on the experiments with the apparatus.

Equation		Group	$k_L a_B$ (hr^{-1})	$k_L a_I$ (hr^{-1})	$k_L a_S$ (hr^{-1})
A (*Equation 8*)	$12.61 = k_L a_B + k_L a_I + k_L a_S$	A, B, C	9.06	2.04	1.51
B (*Equation 9*)	$11.10 = k_L a_B + k_L a_I$	A, B, D	9.27	1.83	1.51
C (Equation 10)	$10.57 = k_L a_B + k_L a_S$	A, C, D	9.27	2.04	1.30
D (Equation 11)	$9.27 = k_L a_B$	B, C, D	9.27	1.83	1.30
		Average	9.22	1.94	1.40

From *Table 2*, It can be seen that the pair of $k_L a_B$ values calculated from the tests without the apparatus and with the apparatus are somewhat identical (9.32 and 9.22 hr^{-1}) as well as the pair of the $k_L a_S$ values (1.37 and 1.40 hr^{-1}). These results indicated that the presence of the apparatus in this scale of experiment had no distinctive effect on bubble transfer and free water surface transfer, but it had an effect to raise the $k_L a_T$ value, from 10.69 to 12.61 hr^{-1}. Therefore, this increment certainly came from the oxygen transfer at the inner interface inside the apparatus, representing 18 % enhancement beyond conventional diffused aeration.

3.3.2 Mathematical analysis

According to the experiment results, the total volumetric oxygen transfer coefficient obtained from the aeration tank with apparatus ($k_L a_T^+$) was 12.61 hr^{-1}, the total volumetric oxygen transfer coefficient obtained from the aeration tank without apparatus ($k_L a_T^-$) was 10.69 hr^{-1}, the bubble transfer coefficient ($k_L a_B$) was 9.22–9.32 hr^{-1}, the inner interface transfer coefficient ($k_L a_I$) was 1.94 hr^{-1}, and the free water surface transfer coefficient ($k_L a_S$) was 1.37–1.40 hr^{-1}.

The measured values of the specific interfacial area of inner interface ($a_{I,mea}$) and the specific interfacial area of free surface ($a_{S,mea}$) were determined by *Equation 13* and *Equation 14*. For this study, the volume of tested water was approximately 100 L and the surface areas of the inner interface and the free water surface were approximately

0.1 m^2 and 0.27 m^2, respectively. As a result, the values of $a_{I,mea}$ and $a_{S,mea}$ could be achieved as 1 m^{-1} and 2.7 m^{-1}.

To determine the experimental values of the specific interfacial area of inner interface ($a_{I,exp}$) and the specific interfacial area of free surface ($a_{S,exp}$), the surface mass transfer coefficient ($k_{L,S}$) was precedingly determined from *Equation 19*. The SEM coefficient is generally known as a constant value which is defined as 0.21 [39] whereas the turbulent energy dissipation is nearly fixed because the turbulence generated on water surface by small bubbles is not considerable. In this study, the generated bubbles had an average diameter approximately 3 mm. According to Lee (2018) [34], the turbulent energy dissipation was about 8 x 10^{-2} m^2/s^3 with the bubble diameter ranged from 1 to 3.5 mm. Therefore, the $k_{L,S}$ value was obtained, and the values of $a_{I,exp}$ and $a_{S,exp}$ were then achieved from *Equation 20* and *Equation 21* as 3.41 m^{-1} and 2.41-2.46 m^{-1}, respectively.

It can be seen that the values of $a_{S,mea}$ and $a_{S,exp}$ were somewhat equivalent. Therefore, the calculated $k_{L,S}$ might be reasonable to apply for the specific interfacial area determination of the atmospheric air-water interface, especially for the free water surface. However, the $a_{I,exp}$ was about 3 times higher than the $a_{I,mea}$. This indicated that the apparatus could enhance the air-water interfacial area not only by the contacting surface area of water inside the apparatus or the inner interface but also by the benefit from the air accumulation which increased air residence time in the aeration process.

From *Equation 16*, *Equation 17*, and *Equation 18*, $k_{L,B}$ was determined as 4.62 x 10^{-4} m/s when d_B was 3 mm, and the $a_{B,exp}$ value of 5.54–5.6 m^{-1} could be obtained. From *Equation 22* and *Equation 23*, the specific interfacial areas in the aeration tank with and without the air-water interface enhancer, a_T^+ and a_T^-, were approximately 11.35–11.47 m^{-1} and 7.95–8.06 m^{-1}, respectively. This would lead to, from *Equation 24* and *Equation 25*, the k_L value of 3.1–3.7 x 10^{-4} m/s which also complied with the values from the other research works [41–43].

3.4 Conclusion

In this scale of experiment, it can be concluded that the main oxygen transfer came from the bubble transfer process, accounting for more than 70 % of the total oxygen transfer. The air-water interface enhancer, which was placed near the water surface, can improve the oxygen transfer through the additional contact area between air and water inside the apparatus (inner interface transfer), accounting for 15.4 % of the total oxygen transfer or 18 % enhancement, while maintaining the maximum performance of the bubble transfer and the free water surface transfer.

From mathematical analysis, it was found that the air-water interface enhancer could improve the interfacial area between air and water, not only by the presence of the inner interface but also by the air accumulation inside the apparatus which increased the air residence time in the aeration process.

Chapter 4 – Study of air-water interface enhancer in diffused aeration system

4.1 Introduction

In previous chapters, it was found that a single layer of the air-water interface enhancer was enough for oxygen transfer enhancement in the diffused aeration system. The apparatus could improve the oxygen transfer performance up to 18 % due to the presence of the inner interface. It was effective when placed near the water surface of the 100-litre aeration tank. This apparatus position allowed the effective cooperation of the oxygen transfer processes from different pathways. However, the position of the air diffuser in the mentioned experiment was focused only on the bottom of the aeration tank. It should be noted that as the submergence depth of the diffuser increases, the energy required to drive air through the diffusers also increases. Therefore, it will be beneficial in terms of energy consumption if the diffuser can be placed farther above the floor of the aeration tank when the aeration system cooperates with the air-water interface enhancer. Moreover, it is also necessary to determine about upscaling in order to apply this apparatus in the actual aeration tank in the wastewater treatment plant. Therefore, the tank geometry was chosen to study as the variable that affected the oxygen transfer process in the aeration system with and without the apparatus. In this study, the tank geometry was considered basically as the volume of the aeration tank (or the water volume) and the depth of the aeration tank (or the water depth).

In experimental sessions, there are a lot of variables related to oxygen transfer which were separately investigated in each experiment. To integrate all factors to determine the volumetric oxygen transfer coefficient, the knowledge of experimental data analysis can be applied to develop the empirical models as design guidelines for aeration systems equipped with the proposed air-water interface enhancer. The models were developed by dimensionless parameters as correlations between volumetric oxygen transfer coefficient and diffused aeration characteristics such as cross-sectional

area of the aeration tank, water depth, diffuser submergence depth, distance of the apparatus above the diffuser, and air flow rate.

The objectives of this chapter were to

(1) study the effect of the diffuser submergence depth and the position of the air-water interface enhancer above the air diffuser on oxygen transfer process in different air flow rates.

(2) study the effect of upscaling factors (water volume and water depth) on the oxygen transfer process equipped with the air-water interface enhancer.

(3) develop the empirical models for determining volumetric oxygen transfer coefficient as design guidelines for aeration systems.

4.2 Materials and method

4.2.1 Experimental setup

In general, the experiment was carried out in the similar setup as in Chapter 2 (*Figure 5*). For determining the effect of diffuser submergence depth and distance of apparatus above diffuser, the position of the air diffuser and the position of the air-water interface enhancer were varied. *Figure 14* shows the variation of the installation of the air-water interface enhancer and the air diffuser in the 100-litre aeration tank. The position of diffuser was indicated as the diffuser submergence depth (h_d) which was the distance of the diffuser below the water surface. Whereas the position of the apparatus was indicated by its distance above the diffuser (h_a). It should be noted that the variety of positions of the apparatus was limited by the position of the diffuser.

Figure 15 shows the experimental setup for determining the effect of the water volume and the water depth. The air-water interface enhancer was installed near the water surface above an air diffuser, which can generate approximately 3-4 mm in diameter of bubbles in tap water (water density; $\rho_w \approx 997$ kg/m^3). There were two aeration tanks used. The first tank (hereafter referred as the lab-scale tank) has a dimension of 30 cm wide by 90 cm long by 55 cm high. The water depth (H) in this tank was set as 37 cm. The second tank (hereafter referred as the pilot-scale tank) has a dimension of 80 cm wide by 80 cm long by 160 cm high. This tank was tested with

tap water at three depths as 60, 80, and 120 cm. Three types of an air pump (17, 120, and 215 W), which supplied air (air density; $\rho_g \approx 1.198$ kg/m^3, and oxygen content by weight; $O_W \approx 0.232$) and generated approximate air flow rates of 20, 100, and 200 LPM, were used. The liquid phase was tap water. A DO meter with a response time of 30 s (Horiba OM-51) was used for measuring dissolved oxygen concentration and water temperature. The position of the DO probe was set in the middle of the water depth (H/2).

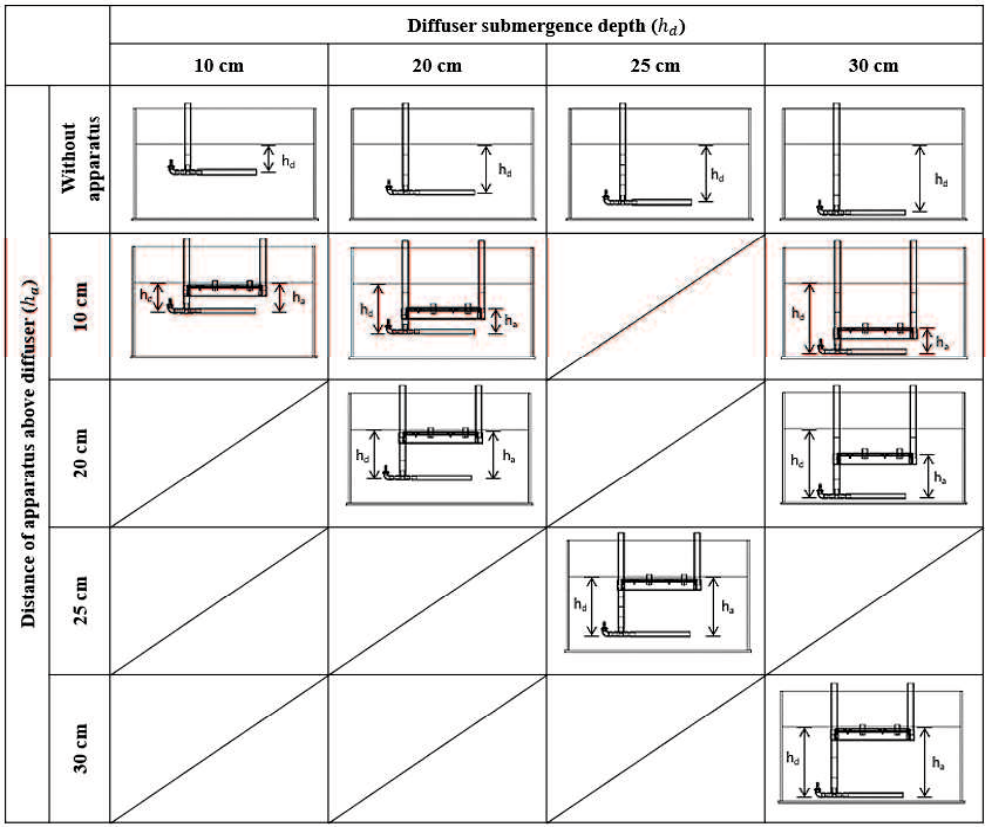

Figure 14 Experimental setups for determining the effect of diffuser submergence depth and distance of apparatus above diffuser.

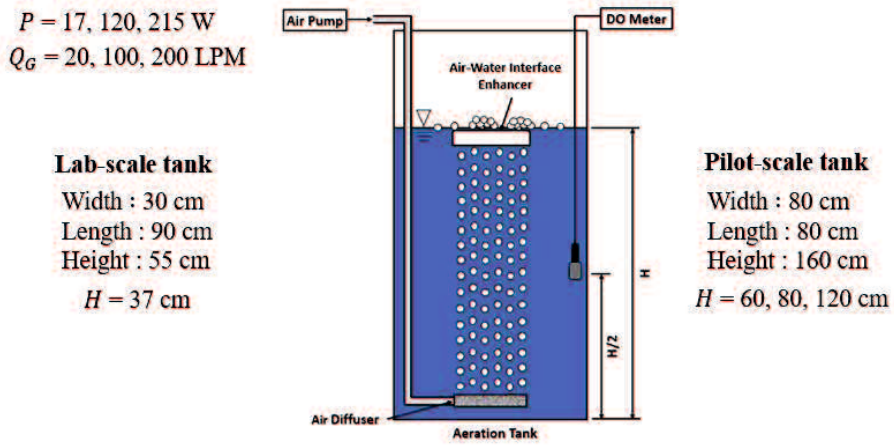

Figure 15 Experimental setup for determining the effect of the water volume and the water depth.

4.2.2 Testing methodology

The oxygen transfer tests were conducted by nitrogen purging method [44]. The dissolved oxygen concentration was initially removed by nitrogen gas injected into tested water in form of bubbles until the dissolved oxygen concentration of water reached nearly 0 mg/L. Then the air was introduced, and the dissolved oxygen concentration and the water temperature were recorded continuously at an interval of 10 s for 20 to 30 min until the oxygen level in the water reached approximately 90 % of the presumed saturated value [25]. The volumetric oxygen transfer coefficient and the standard oxygen transfer rate were determined followed the procedure in *1.5 Analytical oxygen transfer parameters.*

4.2.3 Data analysis

The volumetric oxygen transfer coefficient can be modelled as a function of variables which are tank geometry in terms of cross-sectional area of the aeration tank and water depth, diffuser submergence depth, distance of the apparatus above the diffuser, and air flow rate. In this study, the properties of the liquid related to the oxygen transfer was also included as clean water at standard condition. These properties are diffusivity of oxygen in water, water kinematic viscosity, water density, and water surface tension. The model can be initially expressed as in *Equation 26.*

Equation 26 $$k_L a = f(A_{cs}, H, h_d, h_a, Q_G, D, v_L, \rho_L, \sigma_L)$$

where A_{cs} is the cross-sectional area of the aeration tank, H is the water depth, h_d is the diffuser submergence depth, h_a is the distance of the apparatus above the diffuser, Q_G is the air flow rate, D is the diffusion coefficient of oxygen in water, v_L is the kinematic viscosity of water, ρ_L is the density of water, and σ_L is the surface tension of water. At standard condition with the temperature of 20 °C, D is approximately 2.01 x 10^{-9} m^2/s [36,37], v_L is 1.004 x 10^{-6} m^2/s, ρ_L is 997 kg/m^3 and σ_L is 7.2 x 10^{-2} kg/s^2.

By using dimensional analysis [45–48], these relevant variables were rewritten as dimensionless parameters which are Sherwood number (Sh), Froude number (Fr), Weber number (We), and Reynolds number (Re).

In case of the aeration process without the air-water interface enhancer, the dimensionless parameters were proposed as in *Equation 27* to *Equation 30.* The superficial velocity of air (U_G; where $U_G = Q_G/A_{cs}$) was used for the characteristic velocity and the diffuser submergence depth (h_d) was used for the characteristic length.

Equation 27 $$Sh = \frac{k_L a \cdot h_d \cdot H}{D}$$

Equation 28 $$Fr = \frac{U_G}{\sqrt{g \cdot h_d}}$$

Equation 29 $$We = \frac{U_G^2 \cdot h_d \cdot \rho_L}{\sigma_L}$$

Equation 30 $$Re = \frac{U_G \cdot h_d}{v_L}$$

The relationship of these parameters was expressed with constants as follows.

Equation 31 $$Sh = n \cdot Fr^{\beta_1} \cdot We^{\beta_2} \cdot Re^{\beta_3}$$

In case of the aeration process with the air-water interface enhancer, the dimensionless parameters were proposed as same as in the process without apparatus.

However, the oxygen transfer in this condition not only relied on the diffuser submergence depth (h_d) but also depended on the distance of the apparatus above the diffuser (h_a) as well. Therefore, h_a was additionally included as the characteristic length in the analysis in the function of dimensionless parameters as shown in *Equation 32* to *Equation 35.*

Equation 32 $$Sh' = \frac{k_L a \cdot h_a \cdot H}{D}$$

Equation 33 $$Fr' = \frac{U_G}{\sqrt{g \cdot h_a}}$$

Equation 34 $$We' = \frac{U_G^2 \cdot h_a \cdot \rho_L}{\sigma_L}$$

Equation 35 $$Re' = \frac{U_G \cdot h_a}{\nu_L}$$

The relationship of all dimensionless parameters was then proposed with constants as follows.

Equation 36 $$Sh \cdot Sh' = n \cdot Fr^{\beta_1} \cdot Fr'^{\beta_2} \cdot We^{\beta_3} \cdot We'^{\beta_4} \cdot Re^{\beta_5} \cdot Re'^{\beta_6}$$

The non-linear regression analysis was then conducted with the Solver function in Microsoft Excel [49] by minimizing the value of the squared sum of the difference between data and fit values by changing the coefficient n and all exponents β.

4.3 Results and discussion

4.3.1 Effect of positions of the air diffuser and the air-water interface enhancer

Table 4, *Table 5* and *Table 6* represent the volumetric oxygen transfer coefficients ($k_L a$) at the air flow rates of 20, 100, and 200 LPM, respectively. These tables show the similar trends for any tested air flow rate. The results indicated that the more diffuser submergence depth, the more $k_L a$ obtained because the advantage from the hydrostatic pressure and the distance of bubble dispersion caused the beneficial effect for the bubble transfer process.

Considering the effect of the air-water interface enhancer, when the distance of the apparatus above the diffuser was less than the diffuser submergence depth, the apparatus caused the decrease of the $k_L a$ compared to the aeration processes without the apparatus. The apparatus can obstruct the bubble dispersion, especially when the apparatus was close to the diffuser like the situation in this study that the distance of the apparatus above the diffuser was 10 cm. Therefore, it could be said that the decrease of the overall oxygen transfer process was caused by the decrease of the oxygen transfer from the bubble transfer, and the oxygen transfer from the free water surface and the enhancement from the inner interface were not enough to promote the overall oxygen transfer process.

Considering the position of the air-water interface enhancer, the $k_L a$ increased with the distance of the apparatus above the diffuser. Again, this was due to the advantage from the distance of bubble dispersion.

When the diffuser submergence depth was deep enough, in the study at least 25 cm, the air-water interface enhancer could improve the $k_L a$ beyond the normal aeration process when the apparatus was placed as far from the diffuser as the diffuser submergence depth could provide. In another term, the apparatus was placed at the water surface. This range allowed the bubble transfer process to have an effective role, and the oxygen transfer from the free water surface and the inner interface also helped promoting the overall oxygen transfer process.

In conclusion, it is suggested that, in order to apply the air-water interface enhancer in the diffused aeration system, the air diffuser should be placed close to the bottom of the aeration tank whereas the apparatus should be installed near the water surface. *Figure 16* shows the comparison of bubble dispersion from different arrangements.

Table 4 Volumetric oxygen transfer coefficients at the air flow rate of 20 LPM.

		Diffuser submergence depth (h_d)			
		10 cm	20 cm	25 cm	30 cm
Distance of apparatus above diffuser (h_a)	Without apparatus	5.98	7.68	9.83	10.69
	10 cm	4.96	6.47		6.91
	20 cm		7.56		8.35
	25 cm			10.57	
	30 cm				12.61

Table 5 Volumetric oxygen transfer coefficients at the air flow rate of 100 LPM.

		Diffuser submergence depth (h_d)			
		10 cm	20 cm	25 cm	30 cm
Distance of apparatus above diffuser (h_a)	Without apparatus	16.03	23.56	26.99	28.67
	10 cm	12.54	16.92		18.05
	20 cm		19.91		26.64
	25 cm			27.74	
	30 cm				35.02

Table 6 Volumetric oxygen transfer coefficients at the air flow rate of 200 LPM.

		Diffuser submergence depth (h_d)			
		10 cm	20 cm	25 cm	30 cm
Distance of apparatus above diffuser (h_a)	Without apparatus	28.21	41.47	47.4	59.17
	10 cm	16.19	21.43		36.48
	20 cm		42.80		46.56
	25 cm			53.85	
	30 cm				64.50

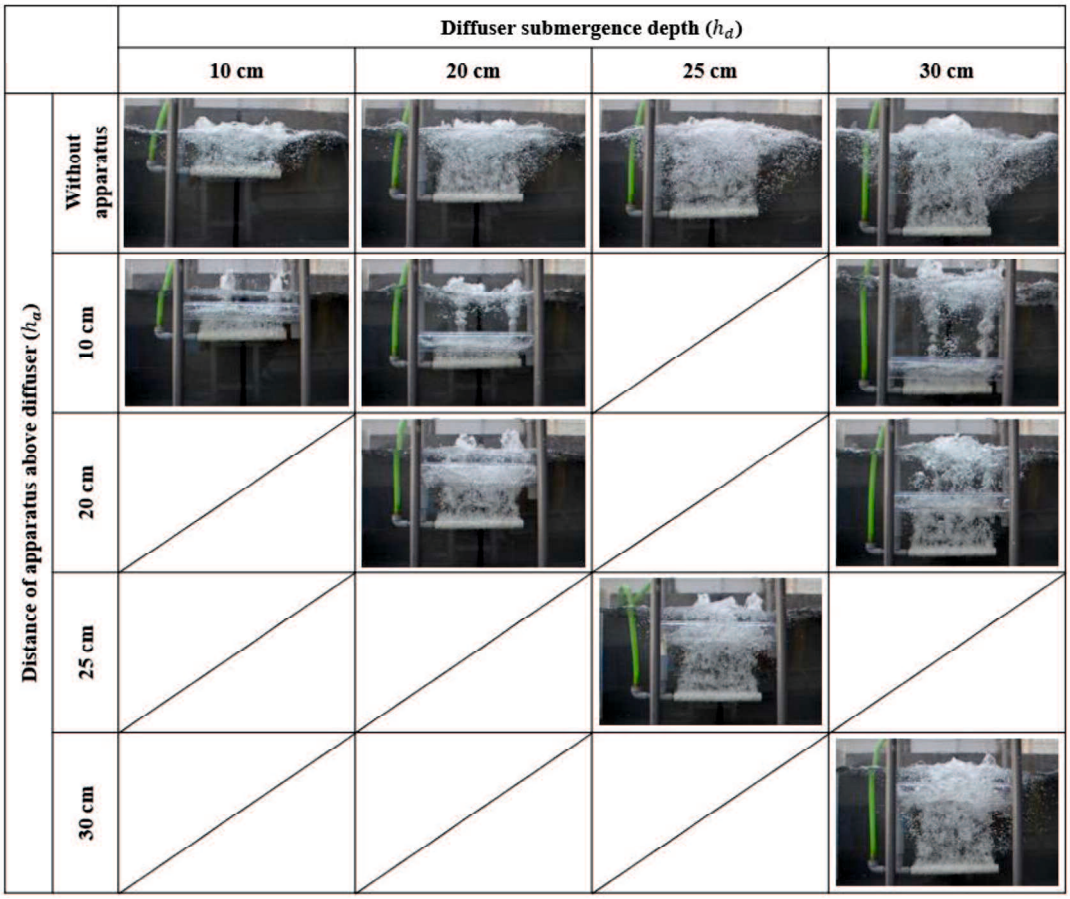

Figure 16 Comparison of bubble dispersion from different arrangements.

4.3.2 Effect of the water volume and the water depth

Considering the air flow rate per water volume (*Figure 17*), the higher rate provided the higher $k_L a$. Moreover, it is obvious that the air-water interface enhancer had the positive effect on the $k_L a$ at high flow rate. Leu et al. (1998) explained that the $k_L a$ increases with the air flow rate because the interfacial mass transfer resistance between the gas and liquid phases is reduced [20].

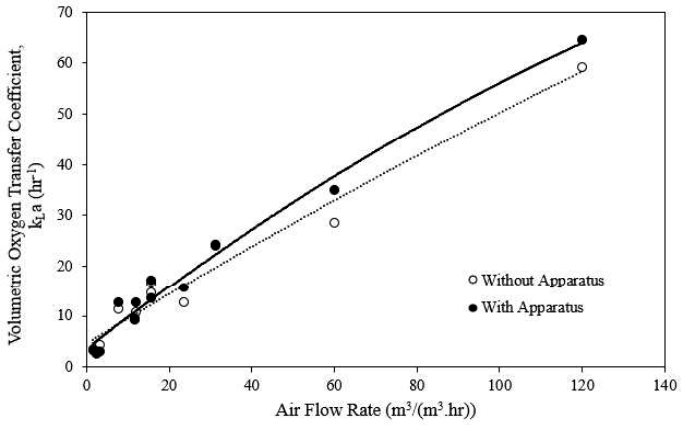

Figure 17 Relationship of volumetric oxygen transfer coefficient and air flow rate per water volume.

From *Figure 18*, the lab-scale tank (100 L) provided higher $k_L a$ than the pilot-scale tank (384-768 L) due to the water volume. For the given air flow rate, the increase of the water volume negatively affected the $k_L a$ because less amount of air supplied per water volume was available for the oxygen transfer process [20].

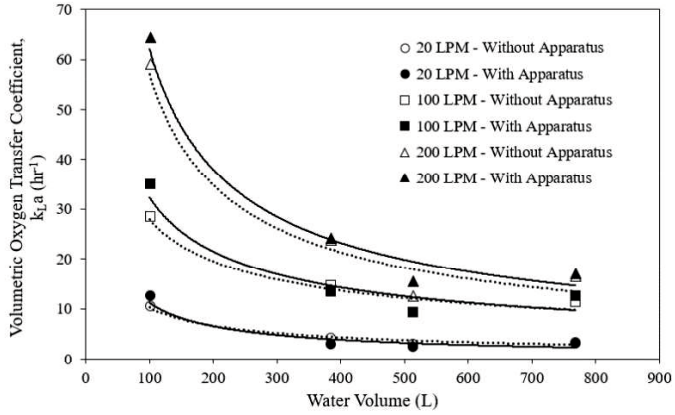

Figure 18 Relationship of volumetric oxygen transfer coefficient and water volume.

Considering the effect of the air-water interface enhancer, there was a clearly positive effect of the apparatus on the $k_L a$ when the air flow rate was 200 LPM. Furthermore, in the lab-scale tank, the apparatus also enhanced the oxygen transfer performance at any tested air flow rates. The scale of the aeration tank also affected the turbulence of the water, which in turn, affected the mixing condition in the aeration system. The turbulence of water or the mixing parameter is often considered as the terms of the velocity gradient [13] which can be calculated by *Equation 37*.

Equation 37

$$G = \sqrt{\frac{P}{\mu V}}$$

where G is the velocity gradient, P is the power input from the air pump, μ is the dynamic viscosity of water ($\mu \approx 8.9 \times 10^{-4}$ kg/m.s). From *Figure 19*, as normal aeration, the velocity gradients in the lab-scale tank were much higher than those in the pilot-scale tank with any water volumes. Therefore, it could be implied that the water turbulence in the lab-scale tank was stronger and could be overcome the obstruction from the air-water interface enhancer which contributed to the reduction of the water turbulence.

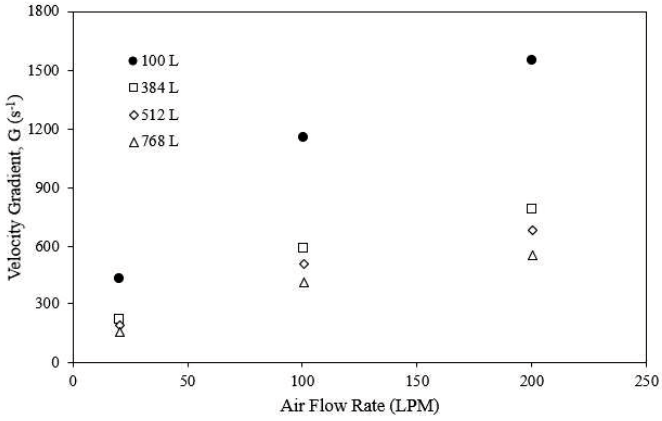

Figure 19 Velocity gradient of water in conventional condition.

Figure 20 shows the volumetric oxygen transfer coefficient regarding the changes of water depth in the pilot-scale tank. Noted that the size of free water surface was always fixed. The result shows the decreasing trends followed by the increasing trends of the $k_L a$ when the water depth increased.

The decrease of the $k_L a$ was due to the fact that the water volume increases with the water depth, which consequently lead to less amount of air supplied per water volume [19,20]. Whereas the increasing trends of $k_L a$ occurred because of water depth leading to high hydrostatic pressure and long rising distance for bubbles which both are highly beneficial to the oxygen transfer process [19,20]. From *Figure 20*, the hydrostatic pressure and the rising distance of bubbles dominated the negative effect of water volume on $k_L a$ in deep water.

In terms of the effect of the air-water interface enhancer, the apparatus seemed unable to enhance the $k_L a$ at low air flow rate. When the air flow rate was higher, there was potential to increase the $k_L a$ especially at high water depth. As a whole, it can be suggested that the oxygen transfer enhancement by the assistance of the apparatus is possible in the deep aeration tank at high air flow rate.

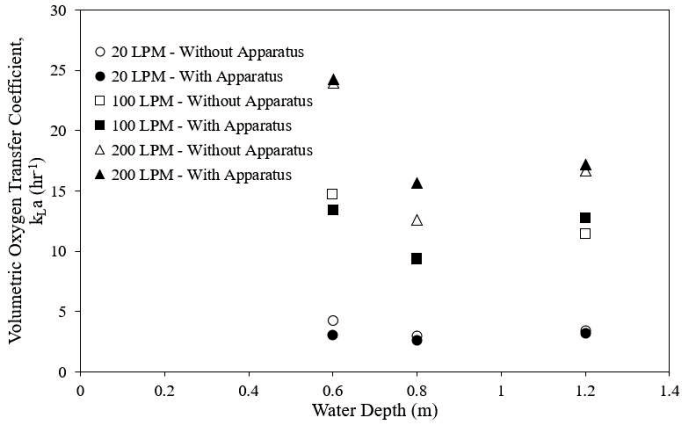

Figure 20 Relationship of volumetric oxygen transfer coefficient and water depth in pilot-scale tank.

From *Figure 21*, it can be seen that the $SOTR$ values generally increased with water volume. The $SOTR$ itself is directly proportional to either $k_L a$ or water volume since the saturated oxygen concentration in water at 20 °C is constant. It is noticeable that even though the water volume of 100 L provided the greatest values of $k_L a$ (*Figure 18*), it provided the lowest $SOTR$ values among other water volumes. Similar to the case of $k_L a$, the effective use of the air-water interface enhancer was observed when the air flow rate was high enough to overcome the obstruction from the apparatus on water turbulence.

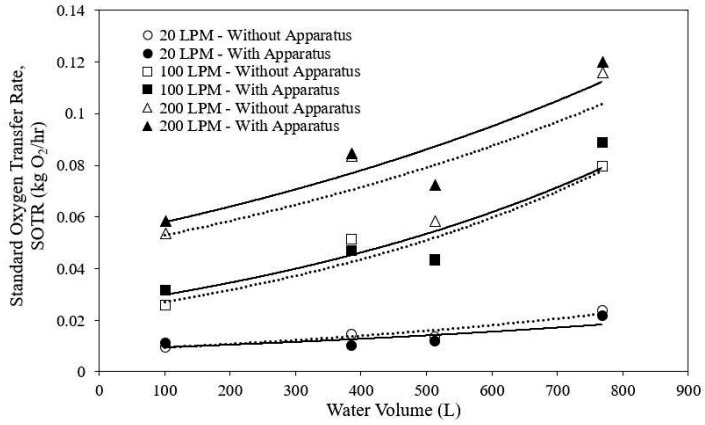

Figure 21 Relationship of standard oxygen transfer rate and water volume.

4.3.3 Data analysis

By performing the Solver function in Microsoft Excel program [49], the adjustable coefficient n and all exponents β could be obtained. In the process without the air-water interface enhancer, the coefficient and exponents were approximately determined as $n \approx 0.78$, $\beta_1 \approx -0.41$, $\beta_2 \approx -0.17$, and $\beta_3 \approx 1.41$ with the error of ±40 % (*Figure 22*). The exponents were substituted, and each variable was rearranged and separated. *Equation 38*, therefore, would be obtained.

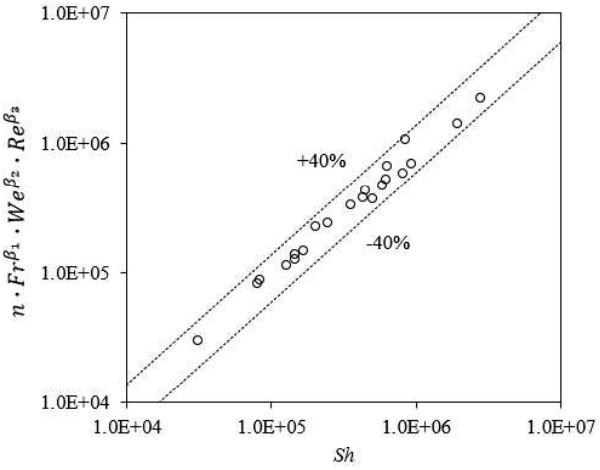

Figure 22 Correlation of the volumetric oxygen transfer coefficients to dimensionless parameters for the process without the air-water interface enhancer.

Equation 38 $$k_L a = nQ_G^{0.67} A_{cs}^{-0.67} h_d^{0.5} H^{-1} g^{0.21} \rho_L^{-0.17} \sigma_L^{0.17} v_L^{-1.41} D$$

To more quickly determine $k_L a$ for design purposes, *Equation 38* could be simplified into the following equation.

Equation 39 $$k_L a = 561.15 \times \left(\frac{Q_G}{A_{cs}}\right)^{0.67} \frac{h_d^{0.5}}{H}$$

where $k_L a$ is in [hr^{-1}], Q_G is in [m^3/s], A_{cs} is in [m^2], h_d is in [m], and H is in [m]. The coefficient of 561.15, which is in [$(1/3600)(m^{-0.17})(s^{-0.33})$], includes the previously determined n, g, and the property values, ρ_L, σ_L, v_L, and D, at 20 °C.

By performing the same method on the process with the air-water interface enhancer, the coefficient n and all exponents β were approximately determined as $n \approx 1.7$, $\beta_1 \approx -0.61$, $\beta_2 \approx -0.79$, $\beta_3 \approx 1.49$, $\beta_4 \approx -1.23$, $\beta_5 \approx -0.19$, and $\beta_6 \approx 2.59$ with the error of ±40 % (*Figure 23*). The exponents were substituted, and each variable was rearranged and separated. *Equation 40*, therefore, would be obtained.

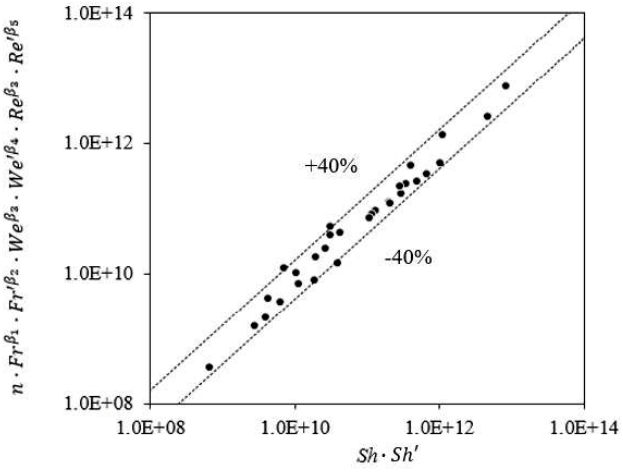

Figure 23 Correlation of the volumetric oxygen transfer coefficients to dimensionless parameters for the process with the air-water interface enhancer.

Equation 40 $$k_L a = n^{0.5} Q_G^{0.77} A_{cs}^{-0.77} h_a^{0.38} h_d^{0.3} H^{-1} g^{0.35} \rho_L^{0.13} \sigma_L^{-0.13} v_L^{-1.2} D$$

Again, for more quickly $k_L a$ determination for design purposes, *Equation 40* could be simplified into the following equation.

Equation 41

$$k_L a = 1143.32 \times \left(\frac{Q_G}{A_{cs}}\right)^{0.77} \frac{h_a^{0.38} h_d^{0.3}}{H}$$

where $k_L a$ is in [hr^{-1}], Q_G is in [m^3/s], A_{cs} is in [m^2], h_a is in [m], h_d is in [m], and H is in [m]. The coefficient of 1143.32, which is in [$(1/3600)(m^{-0.45})(s^{-0.23})$], includes the previously determined n, g, and the property values, ρ_L, σ_L, v_L, and D, at 20 °C.

Figure 24 shows the validation of the proposed models in this study. It can be seen that the trends of estimated $k_L a$ from the models are below the experimental data at high values of $k_L a$. The underestimated values of $k_L a$ are found at the experiment conditions which were conducted in lab-scale at high flow rates. As discussed in *4.3.2 Effect of the water volume and the water depth*, such scale of the tank can provide strong turbulence, especially in high air flow rate conditions where the turbulence is even stronger. Therefore, the probe of the DO meter was highly affected by the strong turbulence of bubbles during aeration. Bubbles could disturb the precision of measurement so that the probe might not be able to distinguish the difference between oxygen from direct bubbles and oxygen dissolved in water. Moreover, the configuration of the lab-scale tank does not proportional to the pilot-scale tank. Therefore, it could be implied that these conditions might lead to some inaccuracy for obtaining experimental results and, in consequence, for developing empirical models.

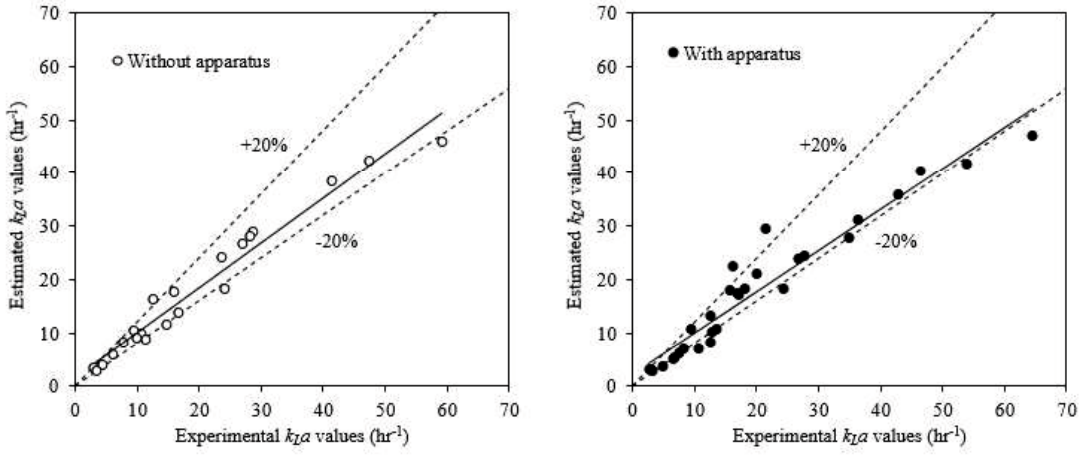

Figure 24 Validation of proposed models for the aeration system in this study.

By applying these models, *Figure 25* to *Figure 29* show the volumetric oxygen transfer coefficients at certain conditions in terms of air flow rate, cross-section area

of the aeration tank, water depth, diffuser submergence depth, and distance of the apparatus above the diffuser. It was found that the air-water interface enhancer could effectively improve the oxygen transfer at high air flow rate. In terms of aeration tank configurations, it was also established that the effectiveness of oxygen transfer enhancement decreased with cross-sectional area of the aeration tank, whereas it increased with water depth, diffuser submergence depth, and distance of the apparatus above the diffuser. Finally, it should be noted that the application of these proposed models is based on the limitation of air diffuser type, the range of air flow rate, and the number of air distribution source. In this study, a tubular stone-type diffuser with 3 cm in diameter and 30 cm long was used. Therefore, these models might not be applicable with other diffuser types because of the influence of different diffuser on bubble characteristic. Moreover, the models are limited for the air flow rate of 20 – 200 LPM. And only one-point source of the air distributor.

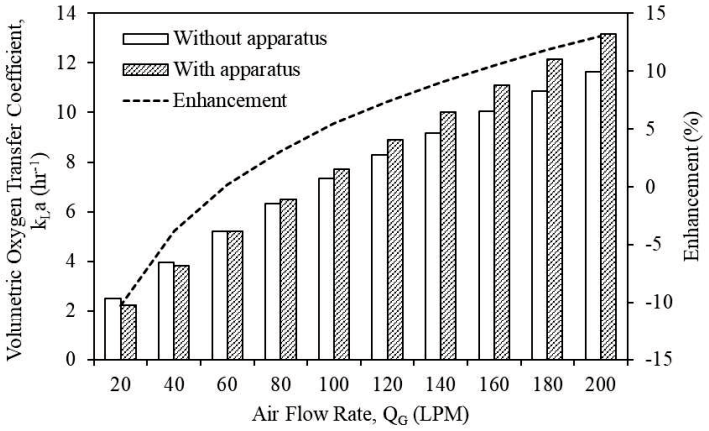

Figure 25 Volumetric oxygen transfer coefficients from proposed models following various air flow rates. A_{cs} = 1 m^2, H = 1 m, h_d = H - 0.1 m, h_a= h_d.

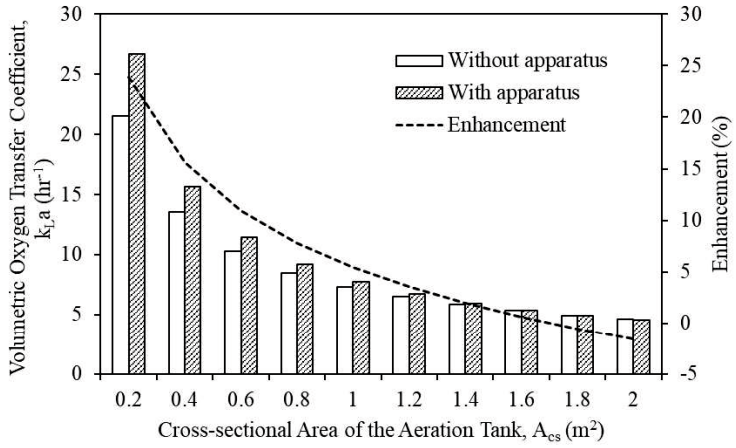

Figure 26 Volumetric oxygen transfer coefficients from proposed models following various cross-sectional areas of the aeration tank. Q_G = 1.7 x 10^{-3} m^3/s, H = 1 m, h_d = H - 0.1 m, h_a= h_d.

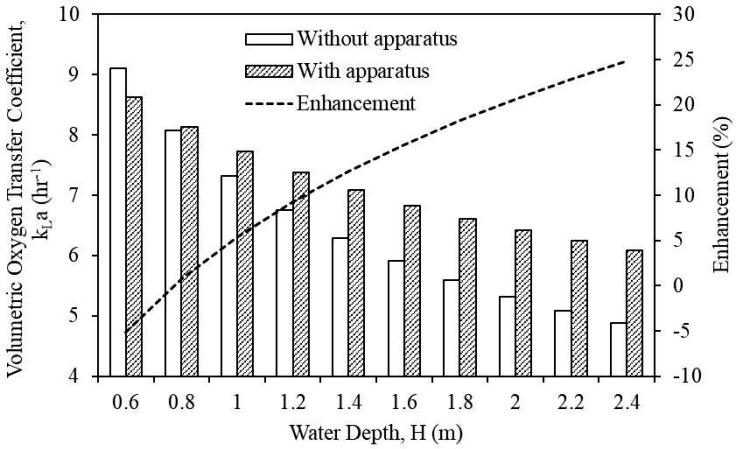

Figure 27 Volumetric oxygen transfer coefficients from proposed models following various water depth. Q_G = 1.7 x 10^{-3} m^3/s, A_{cs} = 1 m^2, h_d = H - 0.1 m, h_a= h_d.

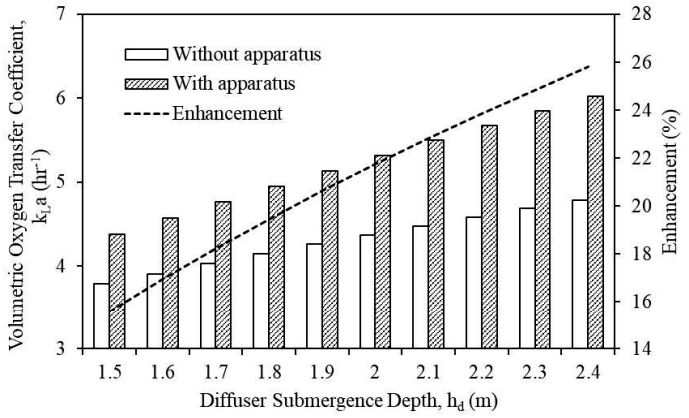

Figure 28 Volumetric oxygen transfer coefficients from proposed models following various diffuser submergence depths. Q_G = 1.7 x 10^{-3} m^3/s, A_{cs} = 1 m^2, H = 2.5 m, h_a= h_d.

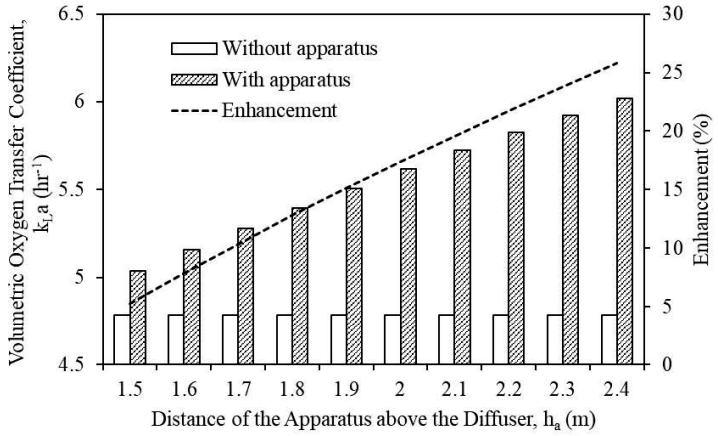

Figure 29 Volumetric oxygen transfer coefficients from proposed models following various distances of the apparatus above the diffuser. Q_G = 1.7 x 10^{-3} m^3/s, A_{cs} = 1 m^2, H = 2.5 m, h_d = H - 0.1 m.

4.4 Conclusion

The diffuser submergence depth had the important role on the oxygen transfer process due to the advantage from the hydrostatic pressure and the distance of bubble dispersion leading to the beneficial effect for the bubble transfer process, whereas the air-water interface enhancer should be installed as far from the diffuser as the diffuser submergence depth could provide which allowed the effective role from the bubble transfer process and the assistance from the free water surface and the inner interface. However, the presence of the inner interface was not enough to improve the overall oxygen transfer performance when the apparatus was placed too close to the air diffuser.

In terms of upscaling factors or tank geometry, there was the compensation between water volume and water depth affecting the k_La, and the negative effect of water volume could be overcome by the increase of hydrostatic pressure and rising distance of bubbles resulted from the water depth, whereas the oxygen transfer enhancement by the assistance of the air-water interface enhancer was possible in the deep aeration tank when the extent of air flow rate was sufficiently high to overcome the obstruction from the apparatus on water turbulence.

Regarding the experimental data, two empirical models for determining the volumetric oxygen transfer coefficient could be developed, one for the conventional aeration system and another for the aeration system with the air-water interface enhancer. These models showed slightly underestimated trend to the experimental results at high volumetric oxygen transfer coefficients. By applying the models, they predicted that the apparatus effectively enhanced the oxygen transfer at high air flow rate. It was also established that the effectiveness decreased with cross-sectional area of the aeration tank, but increased with water depth, diffuser submergence depth, and distance of the apparatus above the diffuser.

Chapter 5 – Application of air-water interface enhancer in diffused aeration system with two aeration units

5.1 Introduction

In previous chapters, the study was so far concentrated on only one-point source of air distributor which can cause the limitation of the distribution of bubble plume in the large scale of the aeration tank. The number of air diffusers and their arrangement have an important influence on bubble dispersion and water circulation in the aeration system, which in turn, affect the oxygen transfer performance and efficiency. Therefore, the number of air diffuser was investigated in this chapter. Moreover, the combination of the air diffuser and the air-water interface enhancer installed near the water surface above the air diffuser, which was defined as the aeration unit, was also investigated for oxygen transfer improvement.

The purposes of this chapter were to

(1) compare the effect of the number of the air diffuser on volumetric oxygen transfer coefficient ($k_L a$) and standard aeration efficiency (SAE) between one aeration unit and two aeration units.

(2) determine the favorable conditions for oxygen transfer considered by the oxygen transfer performance, oxygen transfer efficiency, and oxygen transfer enhancement by the presence of the air-water interface enhancer.

(3) develop empirical models for determining volumetric oxygen transfer coefficient as design guidelines for the aeration tank with multiple aeration units.

5.2 Materials and method

5.2.1 Experimental setup

Figure 30 shows the experimental setup for determining the effect of the number of aeration unit. The experiments were conducted in the pilot-scale tank which has a dimension of 80 cm wide by 80 cm long by 160 cm high. The aeration process was tested with tap water (water density; $\rho_w \approx 997$ kg/m^3) at three depths as 60, 80,

and 120 cm. The different number of aeration unit, one and two units, was observed. The aeration unit is composed of an air diffuser which can generate approximately 3-4 mm in diameter of bubbles in tap water, and an air-water interface enhancer installed near the water surface above the air diffuser when its effect was investigated. Three types of an air pump (17, 120, and 215 W), which supplied air (air density; $\rho_g \approx 1.198$ kg/m^3, and oxygen content by weight; $O_W \approx 0.232$) and generated approximate air flow rates of 20, 100, and 200 LPM, were used. A DO meter with a response time of 30 s (Horiba OM-51) was used for measuring dissolved oxygen concentration and water temperature. The position of the DO probe was set in the middle of the water depth (H/2).

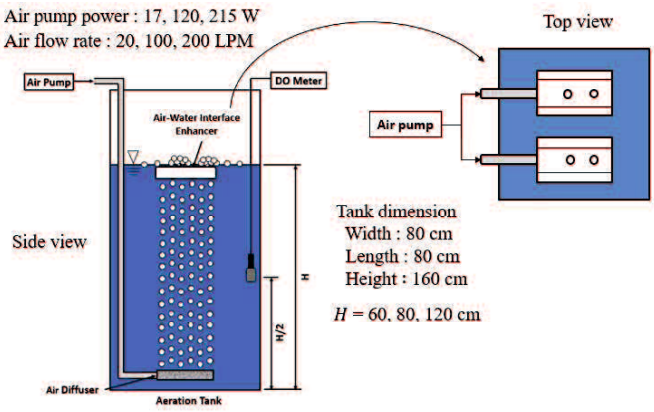

Figure 30 Experimental setup for determining the effect of the number of aeration unit.

5.2.2 Testing methodology

The oxygen transfer tests were conducted by nitrogen purging method [44]. The dissolved oxygen concentration was initially removed by nitrogen gas injected into tested water in form of bubbles until the dissolved oxygen concentration of water reached nearly 0 mg/L. Then the air was introduced, and the dissolved oxygen concentration and the water temperature were recorded continuously at an interval of 10 s for 20 to 30 min until the oxygen level in the water reached approximately 90 % of the presumed saturated value [25]. The volumetric oxygen transfer coefficient and the standard oxygen transfer rate were determined followed the procedure in *1.5 Analytical oxygen transfer parameters*.

5.2.3 Data analysis

The proposed empirical models from Chapter 4 (*Equation 39* and *Equation 41*) were used as basic equations for developing empirical models applied in the aeration tank with multiple aeration units. To include the number of aeration unit (N) in equations, the term of N^{α} was additionally included as the coefficient of the basic equations where α is the adjustable exponent. Therefore, *Equation 39* could be derived into *Equation 42*, and *Equation 41*, where the term of h_a in this case is equal to h_d because the apparatus is placed at the water surface, could be derived into *Equation 43*. These equations were expected to be applied for aeration processes with multiple aeration units by utilizing the data obtained from the tests with one aeration unit and two aeration units.

Equation 42 $$k_L a = N^{\alpha} \times 561.15 \times \left(\frac{Q_G}{A_{cs}}\right)^{0.67} \frac{h_d^{0.5}}{H}$$

Equation 43 $$k_L a = N^{\alpha} \times 1143.32 \times \left(\frac{Q_G}{A_{cs}}\right)^{0.77} \frac{h_d^{0.68}}{H}$$

The values of adjustable exponent α in both equations could be obtained by performing non-linear regression analysis [49] from the experimental data of one aeration unit and two aeration units. To do so, the variable N in *Equation 42* and *Equation 43* was substituted corresponding to the number of the aeration unit.

In case of aeration tests without the air-water interface enhancer, equations for one aeration unit and two aeration units could be obtained as followed.

Equation 44 $$k_L a = 1^{\alpha} \times 561.15 \times \left(\frac{Q_G}{A_{cs}}\right)^{0.67} \frac{h_d^{0.5}}{H}$$

Equation 45 $$k_L a = 2^{\alpha} \times 561.15 \times \left(\frac{Q_G}{A_{cs}}\right)^{0.67} \frac{h_d^{0.5}}{H}$$

In case of aeration tests with the air-water interface enhancer, equations for one aeration unit and two aeration units could be obtained as followed.

Equation 46 $$k_L a = 1^{\alpha} \times 1143.32 \times \left(\frac{Q_G}{A_{cs}}\right)^{0.77} \frac{h_d^{0.68}}{H}$$

Equation 47 $$k_L a = 2^{\alpha} \times 1143.32 \times \left(\frac{Q_G}{A_{cs}}\right)^{0.77} \frac{h_d^{0.68}}{H}$$

5.3 Results and discussion

5.3.1 Effect of the number of aeration unit

Figure 31 shows the results obtained from investigating the different number of aeration unit on oxygen transfer process in the pilot-scale tank. The results provided volumetric oxygen transfer coefficient and standard aeration efficiency for both without and with apparatus conditions. The favorable conditions for oxygen transfer were considered by three aspects, which are oxygen transfer performance in terms of volumetric oxygen transfer coefficient ($k_L a$), oxygen transfer efficiency in terms of standard aeration efficiency (SAE), and oxygen transfer enhancement by the presence of the air-water interface enhancer. The numerical data were classified into categorical data based on available experimental results (*Table 7*) to indicate the most favorable condition for the improvement of the oxygen transfer with the application of the air-water interface enhancer.

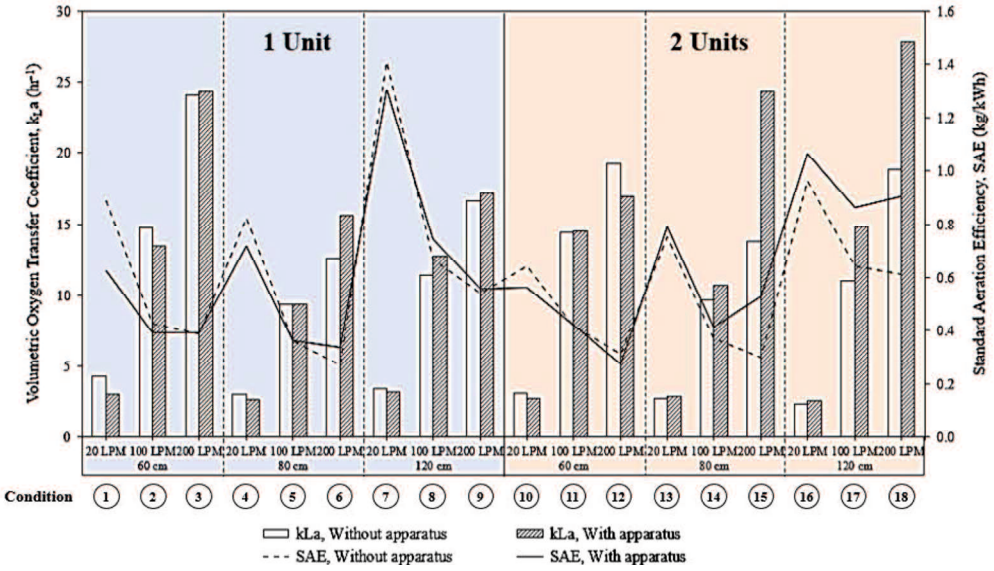

Figure 31 Comparison results between one aeration unit and two aeration units.

Table 7 Result categorization.

Condition	NO. of aeration unit	Water depth (cm)	Air flow rate (LPM)	Oxygen transfer performance	Oxygen transfer efficiency	Oxygen transfer enhancement
1	1	60	20	low	high	no enhancement
2	1	60	100	intermediate	low	no enhancement
3	1	60	200	very high	low	very low
4	1	80	20	very low	high	no enhancement
5	1	80	100	low	very low	no enhancement
6	1	80	200	high	very low	high
7	1	120	20	low	very high	no enhancement
8	1	120	100	intermediate	intermediate	intermediate
9	1	120	200	high	intermediate	low
10	2	60	20	low	intermediate	no enhancement
11	2	60	100	high	intermediate	very low
12	2	60	200	high	very low	no enhancement
13	2	80	20	very low	high	low
14	2	80	100	intermediate	low	intermediate
15	2	80	200	very high	low	very high
16	2	120	20	very low	very high	intermediate
17	2	120	100	intermediate	high	high
18	2	120	200	very high	high	very high

From *Figure 31*, the $k_L a$ increased with air flow rate whereas the SAE decreased with air flow rate except when the oxygen transfer enhancement from the apparatus effectively occurred when two aeration units was operated at 200 LPM in 80 or 120 cm of water depth. Regarding the water depth, the SAE seemingly increased with water depth unlike the $k_L a$. The decrease of $k_L a$ before the increment was observed when the water depth increased except the case of two aeration units with the apparatus at 200 LPM of air flow rate where $k_L a$ apparently increased with water depth. For oxygen transfer enhancement, the apparatus seemed to be positively effective when the aeration process was operated at high air flow rate, in deep water, or with two aeration units.

Regarding the number of the aeration unit, when the aeration process was investigated without the air-water interface enhancer, most of $k_L a$ and SAE were generally somewhat unchanged. However, they slightly decreased at 20 LPM of air flow rate in any water depth and apparently decreased at 200 LPM in 60-cm-deep water. The addition of air diffuser was expected to be beneficial for oxygen transfer in terms of bubble dispersion when compared with using one diffuser, but practically, there was a drawback from the reduction of air flow rate per unit of air diffuser due to the same amount of air supplied. The deterioration of air flow rate causes the high interfacial mass transfer resistance between the gas and liquid phases [20]. As the result, the overall oxygen transfer process was deteriorated especially at low air flow rate as such 20 LPM where bubble dispersion was very weak. Nevertheless, the decrease of oxygen transfer at the air flow rate of 200 LPM in 60-cm-deep water was possibly caused by the coalescence of bubbles. The additional air distribution source not only promotes bubble dispersion, but also increases bubble collision rate. When bubbles collide, they coalesce into larger bubbles which induce the depletion of interfacial area and contact time, which in turn, weaken oxygen transfer process. The high rates of bubble collision and bubble coalescence are possible in the turbulent operation in such system with small volume of water and high air flow rate [50].

When the apparatus was applied, the increase of the number of aeration unit could improve the oxygen transfer process, especially at the air flow rates of 100 and 200 LPM in the water depths of 80 and 120 cm. The additional air-water interface

enhancer could increase the area of inner interface and the volume of air accumulation inside the apparatus. However, it should be noted that the apparatus could not improve the oxygen transfer by low air flow rate which could not overcome the obstruction of the apparatus resulting in poor bubble dispersion as discussed in Chapter 2. Moreover, the increase of hydrostatic pressure and rising distance of bubbles by means of the increase of water depth could be beneficial to the whole oxygen transfer process as discussed in Chapter 4. Therefore, in the conditions with high air flow rates (as 100 and 200 LPM) and deep water (as 80 and 120 cm), the improvement of oxygen transfer could possibly be found.

From *Table 7*, the most favorable condition was Condition 18 (two aeration units in 120-cm-deep water at 200 LPM of air flow rate). This condition provided significantly high degree of oxygen transfer enhancement by the presence of the air-water interface enhancer and high values of $k_L a$ and SAE as well. There were also some conditions which should not be overlooked such as Conditions 8, 15, and 17. Condition 8 provided intermediate degree of all aspects. Condition 15 provided very high oxygen transfer performance and enhancement but low efficiency. Condition 17 provided high oxygen transfer efficiency and enhancement with acceptable oxygen transfer performance.

On the contrary, there were some conditions that provided outstanding oxygen transfer performance or efficiency. However, when considering all mentioned oxygen transfer aspects, unacceptable extent was found. For example, in Condition 3, the air-water interface enhancer could hardly improve oxygen transfer process despite high oxygen transfer performance. Condition 7 provided distinctive efficiency but there was no oxygen transfer improvement from the air-water interface enhancer. High oxygen transfer efficiency was also found in Condition 16, however, oxygen transfer performance was very low.

5.3.2 Empirical model development for multiple aeration units

By performing the Solver function in Microsoft Excel program [49], the adjustable exponents α for the aeration tests in *Equation 44* to *Equation 47* could be

obtained. The exponents α were approximately determined as -0.0132 and 0.2228 for the tests without and with the air-water interface enhancer, respectively, and the relationship between estimated values and experimental values are shown in *Figure 32*. Therefore, the exponents α in *Equation 42* and *Equation 43* could be fulfilled into *Equation 48* and *Equation 49*, respectively, which are expected to be compatible for estimating the volumetric oxygen transfer coefficients in the aeration process equipped with multiple aeration units.

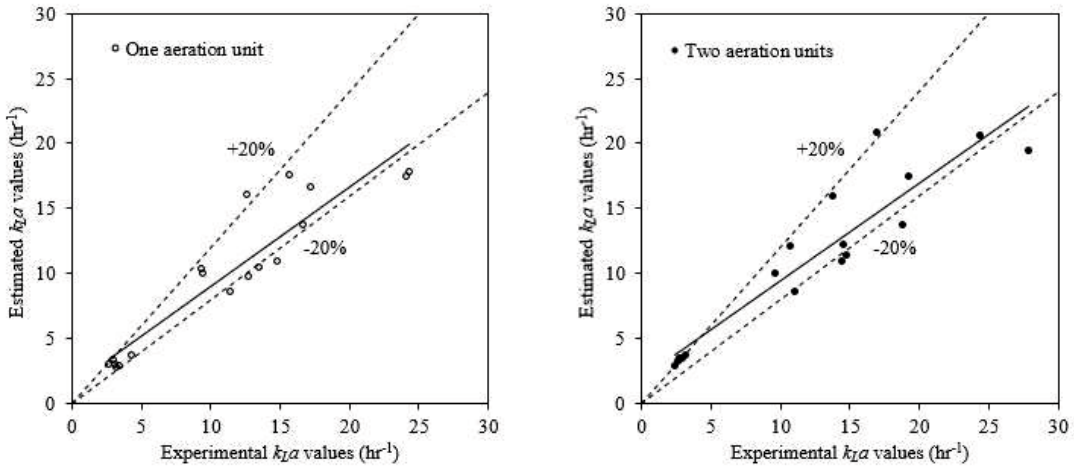

Figure 32 Validation of proposed models for one aeration unit and two aeration units without and with apparatus.

For the aeration process without the air-water interface enhancer,

Equation 48 $$k_L a = N^{-0.0132} \times 561.15 \times \left(\frac{Q_G}{A_{cs}}\right)^{0.67} \frac{h_d^{0.5}}{H}$$

For the aeration process with the air-water interface enhancer,

Equation 49 $$k_L a = N^{0.2228} \times 1143.32 \times \left(\frac{Q_G}{A_{cs}}\right)^{0.77} \frac{h_d^{0.68}}{H}$$

where $k_L a$ is in [hr^{-1}], N is in [-], Q_G is in [m^3/s], A_{cs} is in [m^2], h_d is in [m], and H is in [m].

Figure 33 shows the volumetric oxygen transfer coefficients calculated from *Equation 48* and *Equation 49* from one aeration units up to four aeration units. The

estimation was calculated based on the same scale of the pilot-scale aeration tank in this study. However, the limitation of the models was found showing only decreasing trend of estimated $k_L a$ with water depth because the term of water depth is a denominator of the equations. It can be pointed out that these models do not reflect the consistent results to the experimental data. However, it should be noted that the model development is not based on only experimental data, but also based on theory. The theory indicates that the term of specific interfacial area, a, is volume dependent ($a = A/V$). It means that high water depth, which leads to high water volume, contributes to less specific interfacial area and $k_L a$ as a whole. Moreover, it should be noted that it was mere estimation from the empirical models developed from few sources of data. These proposed models were limited by diffuser type (3-cm in diameter x 30-cm long tubular stone type), air flow rate (20-200 LPM), surface area of the aeration tank (80 cm x 80 cm), and water depth (60-120 cm) based on the experiments. For more precise empirical models, the experiments regarding the size of the aeration tank, the depth of water, and the number of the aeration unit should be further conducted.

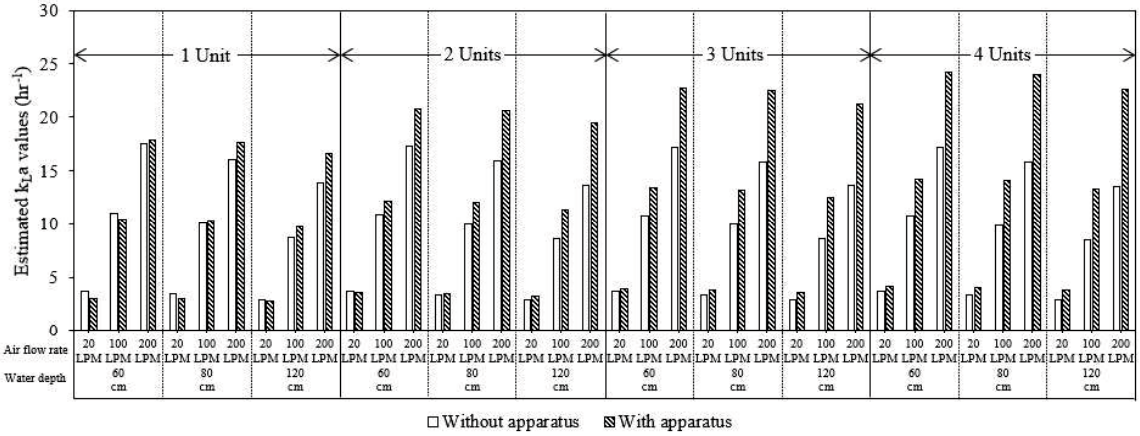

Figure 33 Estimated volumetric oxygen transfer coefficients from the proposed empirical models up to four aeration units.

5.4 Conclusion

In this scale of experiment, the additional installation of the air diffuser seemingly did not have obvious positive effect on the oxygen transfer but $k_L a$ and

SAE values were somewhat unchanged in most conditions or decreased in some conditions. The addition of air diffuser promoted bubble dispersion but the air flow rate per air diffuser also decreased due to the same amount of air supplied, hence, the deterioration of oxygen transfer at low air flow rate. Nevertheless, well distribution of bubble plume also increased bubble collision rate which increased the possibility of bubbles to collide and coalesce into larger bubbles. Therefore, both interfacial area and contact time between air and water decreased causing poor oxygen transfer process.

In terms of the favorable conditions for the application of the air-water interface enhancer, it should be considered by oxygen transfer performance, oxygen transfer efficiency, and oxygen transfer enhancement simultaneously. The installation of two aeration units at 200 LPM in 120 cm deep water provided significantly high degree of oxygen transfer enhancement by the presence of the air-water interface enhancer and high oxygen transfer performance and efficiency as well. This indicated that the installation of air-water interface enhancer as two aeration units could improve the oxygen transfer by increasing the area of inner interface and the volume of air accumulation inside the apparatus in the conditions with high air flow rate and deep water.

Regarding empirical models for determining the volumetric oxygen transfer coefficients in the aeration process with multiple aeration units, two models were developed, one for the aeration process without the apparatus and one for with the apparatus. However, for precise empirical models, the experiments with the variety of the size of the aeration tank, the depth of water, and the number of the aeration unit should be further conducted to collect more experimental data for model development.

Chapter 6 - Summary and recommendations

This work investigated the feasibility of the air-water interface enhancer for effective application to improve the oxygen transfer performance and the oxygen transfer efficiency. The distinct feature of this work is the concept of utilizing the free surface area as the means of oxygen transfer improvement.

The effect of the arrangement of the air-water interface enhancer was preliminarily investigated in terms of volumetric oxygen transfer coefficient and standard oxygen transfer efficiency over the range of air flow rate in the lab-scale aeration tank. It was found that a single layer of apparatus located near the water surface was the optimal arrangement as the available distance between diffuser and apparatus allowed bubble dispersion and the assistance of the apparatus promoted the overall oxygen transfer process.

The assistance of the air-water interface enhancer was investigated in the laboratory scale with optimal arrangement of the apparatus by determining the volumetric oxygen transfer coefficient from different oxygen transfer pathways and by determining the specific interfacial area enhancement. The results concluded that, in this scale of the experiment, the apparatus could increase the oxygen transfer through the inner interface transfer with 18 % enhancement and maintain the maximum performance of bubble transfer and free water surface transfer. From the specific interfacial area determination, the results revealed that the oxygen transfer enhancement occurred not only by the presence of the inner interface but also by the air accumulation inside the apparatus which increased the contact time between air and water in the aeration process.

For the study on the factors related to the diffused aeration process, it was found that the diffuser submergence depth had the important role on the oxygen transfer process. The advantage from the hydrostatic pressure and the distance of bubble dispersion provides the beneficial effect for the bubble transfer process. In this study, even though the diffuser was installed near the floor of the aeration tank, the air-water interface enhancer could not effectively improve the oxygen transfer performance when the apparatus was placed too close to the diffuser causing the

decrease of the oxygen transfer from the bubble transfer. Therefore, the apparatus should be installed as far from the diffuser as the diffuser submergence depth could provide to allow the effective role from the bubble transfer process and the assistance from the apparatus. For the effect of the tank geometry, the water volume and the water depth were investigated in both lab-scale and pilot scale aeration tank over the range of air flow rate. There was the compensation between water volume and water depth affecting the volumetric oxygen transfer coefficient, and the negative effect of water volume could be overcome by the increase of the hydrostatic pressure and the rising distance of bubbles resulted from the water depth. The oxygen transfer enhancement by the presence of the air-water interface enhancer was observed in the deep aeration process with high air flow rate. The results also revealed that the volumetric oxygen transfer coefficient increased whereas the standard oxygen transfer efficiency decreased with air flow rate per water volume.

By applying dimensionless parameters, two empirical models were developed for determining the volumetric oxygen transfer coefficients in the conventional aeration system and the aeration system with the air-water interface enhancer. These models could be applied as design guidelines for diffused aeration systems equipped with the proposed apparatus by deciding the extents of cross-sectional area of the aeration tank, water depth, diffuser submergence depth, distance of the apparatus above the diffuser, and air flow rate.

Finally, two sets of air diffuser and air-water interface enhancer could improve the oxygen transfer by increasing the area of inner interface and the volume of air accumulation inside the apparatus in the conditions with high air flow rate and deep water. The favorable conditions for oxygen transfer was considered by oxygen transfer performance, oxygen transfer efficiency, and oxygen transfer enhancement by the air-water interface enhancer simultaneously. In this scale of study, the most favorable condition was the installation with two aeration units in 120-cm-deep water at 200 LPM of air flow rate which provided significantly high degree of oxygen transfer enhancement by the presence of the air-water interface enhancer and high oxygen transfer performance and efficiency as well. Moreover, the empirical models for aeration process with multiple aeration units were also proposed as design guidelines.

However, the additional experiments were also recommended for more precise estimation.

This study is based on air-water system. However, in actual application, the liquid in the aeration system is different in terms of properties. The wastewater in the activated sludge process contains suspended solids which affect oxygen transfer rate or $k_L a$. Some literatures indicated that this contamination can be expressed as alpha factor ($\alpha - factor = k_L a_{wastewater} / k_L a_{clean\ water}$), which ranges between 0.8-1 at the normal range of suspended solid of 1-3 g/L in the conventional aeration [51–53]. It is possible to apply alpha factor for estimating $k_L a$ in wastewater from the proposed models. However, it should be noted that suspended solids may also cause possible fouling inside the apparatus. Therefore, this issue requires further investigation on the application of the air-water interface enhancer in the aeration process with actual wastewater for precise effect of wastewater on $k_L a$ and the role of the apparatus. Moreover, the apparatus was initially designed for multi-layer arrangement to increase the air-water interface along the depth of the aeration tank. However, in this study, there was a problem about the obstruction from the apparatus which caused the deterioration of bubble dispersion. This was the major concern in the view of the author because the apparatus could not work as well as initial expectation. Therefore, these mentioned issues would lead to the study on apparatus modification aiming to reduce the drawback of the apparatus on bubble flow characteristic. If the study on apparatus modification is successful, further study on multi-layer arrangement in deeper actual aeration tanks would be recommended.

References

[1] McWhirter JR, Hutter JC. Improved oxygen mass transfer modeling for diffused/subsurface aeration systems. AIChE J. 1989;35:1527–1534.

[2] Wilhelms SC, Martin SK. Gas Transfer in Diffused Bubble Plumes. US Army Res. 1992;64.

[3] DeMoyer CD, Schierholz EL, Gulliver JS, et al. Impact of bubble and free surface oxygen transfer on diffused aeration systems. Water Res. 2003;37:1890–1904.

[4] Schaub F, Pluschkell W. Turbulent enhancement of mass transfer in bubble plumes. Chem. Eng. Technol. 2006;29:1073–1083.

[5] Shibata K, Terasaka K, Fujioka S, et al. Oxygen transfer from a free surface and dispersed bubbles in an aeration tank. J. Chem. Eng. Japan. 2016;49:391–398.

[6] Parker SP. McGraw-Hill Dictionary of Scientific and Technical Terms [Internet]. McGraw-Hill Education; 2003. Available from: https://books.google.co.jp/books?id=xOPzO5HVFfEC.

[7] American Meteorological Society. Glossary of Meteorology [Internet]. 2020. Available from: http://glossary.ametsoc.org/wiki/Free_surface.

[8] Zhu H, Imai T, Tani K, et al. Enhancement of oxygen transfer efficiency in diffused aeration systems using liquid-film-forming apparatus. Environ. Technol. 2007;28:511–519.

[9] Zhu H, Imai T, Tani K, et al. Development of High Efficient Oxygen Supply Method by Using Contacting Water-Liquid film with Air. J. Water Environ. Technol. 2007;5:57–69.

[10] Imai T, Zhu H. Improvement of Oxygen Transfer Efficiency in Diffused Aeration Systems Using Liquid-Film-Forming Apparatus. In: Nakajima HZE-H, editor. Rijeka: IntechOpen; 2011. p. 341–370. Available from: https://doi.org/10.5772/22908.

[11] Hongprasith N, Imai T, Painmanakul P. Study of the liquid-film-forming apparatus as an alternative aeration system: design criteria and operating condition. Environ. Technol. 2017;38:1539–1547.

[12] Jamnongwong M, Charoenpittaya T, Hongprasith N, et al. Study of liquid film forming apparatus (LFFA) mechanisms in terms of oxygen transfer and bubble hydrodynamic parameters. Eng. J. 2016;20:77–90.

[13] Mueller JA, Boyle WC, Pöpel HJ. Aeration : Principles and Practice. Boca Raton: CRC Press; 2002.

[14] Jenkins TE. Aeration Control System Design: A Practical Guide to Energy and Process Optimization. John Wiley & Sons; 2013.

[15] Yoshida F, Akita K. Performance of gas bubble columns: Volumetric liquid-phase mass transfer coefficient and gas holdup. AIChE J. 1965;11:9–13.

[16] Kara M, Sung S, Klinzing GE, et al. Hydrogen mass transfer in liquid hydrocarbons at elevated temperatures and pressures. Fuel. 1983;62:1492–1498.

[17] Bavarian F, Linn C-J, Ramesh TS, et al. Effect of Static Liquid Height on Gas-Liquid Mass Transfer in a Draft-Tube Bubble Column and Three-Phase Fluidized Bed. Chem. Eng. Commun. 1991;108:347–364.

[18] Wu WT, Hsiun DY. Oxygen transfer in an airlift reactor with multiple net draft tubes. Bioprocess Eng. 1996;15:59–62.

[19] Chang M-Y, Morsi BI. Solubilities and mass transfer coefficients of carbon monoxide in a gas-inducing reactor operating with organic liquids under high pressures and temperatures. Chem. Eng. Sci. 1992;47:3541–3548.

[20] Leu HG, Lin SH, Shyu CC, et al. Effects of surfactants and suspended solids on oxygen transfer under various operating conditions. Environ. Technol. 1998;19:299–306.

[21] Bando Y, Chaya M, Hamano SI, et al. Effect of liquid height on flow characteristics in bubble column using highly viscous liquid. J. Chem. Eng. Japan. 2003;36:523–529.

[22] ASCE. Measurement of Oxygen Transfer in Clean Water. American Society of Civil Engineers; 2007.

[23] Metcalf & Eddy. Wastewater engineering : treatment and reuse. 4th ed. Boston: McGraw-Hill; 2003.

[24] Qasim SR, Zhu G. Wastewater treatment and reuse: Theory and design examples: Volume 1: Principles and basic treatment. Wastewater Treat. Reuse, Theory Des. Examples Vol. 1 Princ. Basic Treat. Boca Raton: CRC Press; 2017.

[25] APHA. Standard methods for the examination of water and wastewater. 22nd ed. Rice, Eugene W., Baird, Rodger B., Eaton, Andrew D., Clesceri LS, editor. Washington, D.C., USA: American Public Health Association (APHA), American Water Works Association (AWWA) and Water Environment Federation (WEF); 2012.

[26] Terashima M, So M, Goel R, et al. Determination of diffuser bubble size in computational fluid dynamics models to predict oxygen transfer in spiral roll aeration tanks. J. Water Process Eng. 2016.

[27] Amaral A, Bellandi G, Rehman U, et al. Towards improved accuracy in modeling aeration efficiency through understanding bubble size distribution dynamics. Water Res. 2018;131:346–355.

[28] Gresch M, Armbruster M, Braun D, et al. Effects of aeration patterns on the flow field in wastewater aeration tanks. Water Res. 2010;45:810–818.

[29] Kulkarni AA, Joshi JB. Bubble Formation and Bubble Rise Velocity in Gas - Liquid Systems : A Review. 2005;5873–5931.

[30] Kantarci N, Borak F, Ulgen KO. Bubble column reactors. 2005;40:2263–2283.

[31] Cheng X, Xie Y, Zheng H, et al. Effect of the Different Shapes of Air Diffuser on Oxygen Mass Transfer Coefficients in Microporous Aeration Systems. Procedia Eng. 2016;154:1079–1086.

[32] Maneri CC, Mendelson HD. The Rise Velocity of Bubbles in Tubes and Rectangular Channels As Predicted by Wave Theory. 14:295–300.

[33] Treybal RE. Mass-transfer Operations. New York: McGraw-Hill; 1980.

[34] Lee S. Evaluation of oxygen transfer from bubble and free surface in bubble reactors using CFD. Chem. Eng. Res. Des. 2018;140:251–260.

[35] Higbie R. The Rate of Absorption of a Pure Gas into a Still Liquid during Short Periods of Exposure. Trans. AIChE. 1935;31:365–389.

[36] Engineering ToolBox. Diffusion Coefficients of Gases in Water [Internet]. 2008. Available from: https://www.engineeringtoolbox.com/diffusion-coefficients-d_1404.html.

[37] Xing W, Yin M, Lv Q, et al. 1 - Oxygen Solubility, Diffusion Coefficient, and Solution Viscosity. In: Xing W, Yin G, Zhang JBT-REM and ORE, editors. Amsterdam: Elsevier; 2014. p. 1–31.

[38] Lamont JC, Scott DS. An eddy cell model of mass transfer into the surface of a turbulent liquid. AIChE J. 1970;16:513–519.

[39] Wang B, Liao Q, Fillingham JH, et al. On the coefficients of small eddy and surface divergence models for the air-water gas transfer velocity. J. Geophys. Res. Ocean. 2015;120:2129– 2146.

[40] Zappa CJ, McGillis WR, Raymond PA, et al. Environmental turbulent mixing controls on air-water gas exchange in marine and aquatic systems. Geophys. Res. Lett. 2007;34:1–6.

[41] Jamnongwong M, Loubiere K, Dietrich N, et al. Experimental study of oxygen diffusion coefficients in clean water containing salt, glucose or surfactant: Consequences on the liquid-side mass transfer coefficients. Chem. Eng. J. 2010;165:758–768.

[42] Sardeing R, Painmanakul P, Hébrard G. Effect of surfactants on liquid-side mass transfer coefficients in gas-liquid systems: A first step to modeling. Chem. Eng. Sci. 2006;61:6249–6260.

[43] Sastaravet P, Chuenchaem C, Thaphet N, et al. Comparative Study of Mass Transfer and Bubble Hydrodynamic Parameters in Bubble Column Reactor: Physical Configurations and Operating Conditions. Environ. Eng. Res. 2014;19:345–354.

[44] Butler IB, Schoonen MAA, Rickard DT. Removal of dissolved oxygen from water: A comparison of four common techniques. Talanta. 1994;41:211–215.

[45] Al Ba'ba'a HB, Amano RS. A study of optimum aeration efficiency of a lab-scale air-diffused system. Water Environ. J. 2017;31:432–439.

[46] Pittoors E, Guo Y, Van Hulle SWH. Oxygen transfer model development based on activated sludge and clean water in diffused aerated cylindrical tanks. Chem. Eng. J. 2014;243:51–59.

[47] Khudenko BM, Shpirt E. Hydrodynamic parameters of diffused air systems. Water Res. 1986;20:905–915.

[48] Schierholz EL, Gulliver JS, Wilhelms SC, et al. Gas transfer from air diffusers. Water Res. 2006;40:1018–1026.

[49] Brown AM. A step-by-step guide to non-linear regression analysis of experimental data using a Microsoft Excel spreadsheet. Comput. Methods Programs Biomed. 2001;65:191–200.

[50] Prince MJ, Blanch HW. Bubble coalescence and break-up in air-sparged bubble columns. AIChE J. 1990;36:1485–1499.

[51] Krampe J, Krauth K. Oxygen Transfer into Activated Sludge with High MLSS Concentrations. Water Sci. Technol. 2003;47:297–303.

[52] van der Roest HF, van Bentem AGN, Lawrence DP. MBR-technology in municipal wastewater treatment: challenging the traditional treatment technologies. Water Sci. Technol. 2002;46:273–280.

[53] Henkel J. Oxygen Transfer Phenomena in Activated Sludge. 2010.